

1 **Relevance of feedbacks between water availability and crop** 2 **systems using a coupled hydrologically – crop growth model**

3 Sneha Chevuru¹, L.P.H. (Rens) van Beek¹, Michelle T.H. van Vliet¹, Jerom P.M. Aerts^{2&3},
4 Marc F.P. Bierkens^{1&4}

5 1 Department of Physical Geography, Utrecht University, The Netherlands.

6 2 Water Resources Section, Faculty of Civil Engineering and Geosciences, Delft University of Technology, The
7 Netherlands

8 3 Department of Hydraulic Engineering, Faculty of Civil Engineering and Geosciences, Delft University of
9 Technology, The Netherlands

10 4 Unit Subsurface & Groundwater Systems, Deltares, Utrecht, The Netherlands

11
12 *Correspondence to:* Sneha Chevuru (s.chevuru@uu.nl)

13 14 **Abstract**

15 Individual hydrological and crop growth models often oversimplify underlying processes,
16 reducing the accuracy of both simulated hydrology and crop growth dynamics. While crop
17 models tend to generalize soil moisture processes, most hydrological models commonly use
18 constant vegetation parameters and prescribed phenologies, neglecting the dynamic nature of
19 crop growth. Despite some studies that have coupled hydrological and crop models, a limited
20 understanding exists regarding the feedbacks between hydrology and crop growth. Our
21 objective is to quantify the feedback between crop systems and hydrology on a fine-grained
22 spatio-temporal level. To this end, the PCR-GLOBWB 2 hydrological model was coupled with
23 the WOFOST crop growth model to quantify both the one-way and two-way interactions
24 between hydrology and crop growth on a daily timestep and at 5 arc minutes (~10 km)
25 resolution. Our study spans the Contiguous United States (CONUS) region and covers the
26 period from 1979 to 2019, allowing a comprehensive evaluation of the feedback between
27 hydrology and crop growth dynamics. We compare individual (stand-alone) as well as one-
28 way and two-way coupled WOFOST and PCR-GLOBWB 2 model runs and evaluate the
29 average crop yield and its interannual variability for rainfed and irrigated crops as well as
30 simulated irrigation water withdrawal for maize, wheat and soybean. Our results reveal distinct
31 patterns in the temporal and spatial variation of crop yield depending on the included
32 interactions between hydrology and crop systems. Evaluating the model results against
33 reported yield and water use data demonstrates the efficacy of the coupled framework in
34 replicating observed irrigated and rainfed crop yields. Our results show that two-way coupling,
35 with its dynamic feedback mechanisms, outperforms one-way coupling for rainfed crops. This
36 improved performance stems from the feedback of WOFOST crop phenology to the crop
37 parameters in the hydrological model. Our results suggest that when crop models are combined

38 with hydrological models, a two-way coupling is needed to capture the impact of interannual
39 climate variability on food production.

40

41

42 **1 Introduction**

43 Global trends in population and economic growth are expected to increase the demand for
44 water, food, and energy, threatening the sustainable and equitable use of natural resources
45 (Sophocleous, 2004; Tompkins and Adger, 2004). Water as a resource plays a crucial role in
46 crop growth, cooling of thermoelectric plants, hydropower generation, and covering domestic
47 and industrial demand. Water, therefore, is an essential resource at the core of the Water-
48 Energy-Food-Ecosystem (WEFE) nexus. Currently, 70% of total global freshwater
49 withdrawals are accounted for by agriculture, making it the largest water user among all sectors
50 (Dubois, 2011). The Food and Agriculture Organization (FAO) of the United Nations estimated
51 that the demand for water and food resources will likely increase by 50% by 2050 compared
52 to 2015 (IRENA, 2015; Corona-López et al., 2021). The increasing demand for water and food
53 will likely have negative impacts on the environment and will inhibit socio-economic
54 development if a gap opens between growing water demand and water availability.

55 The critical interplay between hydrology and crop growth becomes evident during
56 hydroclimatic extremes (e.g. droughts, heatwaves), as rising demands coincide with potential
57 declines in both water resources and food production (crop yield) (Jackson et al., 2021). In
58 addressing the complexities associated with these challenges, studies by Jägermeyr et al.
59 (2017), utilizing a dynamic vegetation model (LPJmL), evaluated achievable irrigated crop
60 production under sustainable water management. Their findings revealed that 41% of global
61 water use currently compromises environmental flow requirements crucial for river
62 ecosystems, potentially leading to losses in irrigated croplands. Concurrently, research by
63 Vörösmarty et al. (2000) and Leclère et al., (2014) projects the impacts of climate change on
64 global agricultural systems, foreseeing an increase in irrigated areas in the future, underscoring
65 the necessity for significant investments in irrigation, energy, and water resource management.

66 Biophysical process-based models, as highlighted by Siad et al., (2019) and Zhang et al.,
67 (2021), are instrumental in understanding the intricate relationship between hydrology and crop
68 growth, particularly in response to changing hydroclimatic conditions. Considering factors like
69 irrigation water use and soil-groundwater dynamics, these models explore how meteorological

70 events influence water availability for crops, as well as the impacts of diminished growth and
71 premature senescence on hydrology through effects on root water uptake and
72 evapotranspiration. This understanding becomes crucial when assessed at the regional to global
73 scale, where local deficits can have cascading consequences for both water and food security.

74 In the context of studying the impact of climate change and variability on crop yields, aside
75 from biophysical models, numerous crop models have been employed. However, these models
76 often incorporate a simplified soil-water balance (Zhang et al., 2021) that overlooks local
77 hydrological processes and often do not account for water use for irrigation and non-
78 agricultural sectors. Conversely, most hydrological models simplify or neglect the effects of
79 land cover, phenology and vegetation changes on hydrological fluxes and the state of available
80 water resources (Tsarouchi et al., 2014). These simplifications arise due to computational
81 expediency, disparities in process scales between hydrology at the river basin level and crop
82 yield at the field level, incomplete understanding of the other domain by model developers, or
83 because of epistemological uncertainty (Siad et al. 2019; McMillan et al., 2018; Shafiei et al.
84 2014). Recognizing the strengths of both crop models and global hydrological models, a
85 coupling allows for the exploration of dynamic crop growth's influence on hydrology and water
86 use and the incorporation of accurate spatio-temporal variations in hydrological fluxes,
87 including water use, in estimates of crop yield.

88 Noteworthy efforts by Droppers et al. (2021) have successfully coupled hydrological and crop
89 models, primarily focusing on achieving attainable crop production. However, these efforts
90 were conducted at half-degree (~50 km) spatial resolution and focused on long-term average
91 crop yield. They therefore fall short in exploring the aspects of fine-scale spatiotemporal
92 variability in particular as a result of interannual climate variability. Other recent efforts to
93 couple crop growth models and global hydrological models (Jägermeyr et al., 2017)
94 predominantly focus on assessing yield under different scenarios or adaptation measures.
95 However, limited work focused on delving into how two-way interactions and feedback
96 mechanisms between crop growth and hydrological systems operate.

97 In addition, integrated assessment models have been instrumental in studying the combined
98 effects of climate change and socio-economic developments on crop yield and water resources
99 at a large scale. Typically, these models operate on a macro-regional level (Easterling, 1997)
100 and use annual (or 5 to 10 yearly timesteps), neglecting the impacts of inter- and intra-annual
101 variability and particularly short-term hydroclimatic extremes. Furthermore, integrated

102 assessment models often adopt an optimization modelling approach, making them less suitable
103 for studying the effects of hydroclimatic extremes (Ewert et al., 2015).

104 Another class of efforts to link water to crop production are water-food nexus studies, that,
105 however, tend to concentrate on local linkages or provide qualitative descriptions of existing
106 connections (Momblanch et al., 2019). For instance, a recent review of water-food nexus
107 studies focusing on the contiguous United States (CONUS), shows that such studies focus
108 mainly on water security indicators (Veettil et al., 2022) or climate variability impacts on crop
109 yields (Huang et al., 2021). However, knowledge gaps persist, as water and food resources are
110 often evaluated separately (Corona-López et al., 2021), exploring allocations through an
111 optimization model (Mortada et al., 2018) that lacks spatiotemporal variability considerations.
112 Notably, there is a lack of effort to understand the interactions between hydrology and crop
113 growth. Further research is needed to bridge these gaps and enhance our understanding of the
114 dynamic and interlinked processes shaping the water-food nexus.

115 To address this knowledge gap, our objective is, therefore, to quantify the feedback between
116 crop growth and hydrology. Although eventually global scale in scope, we limit this analysis
117 to the Contiguous United States (CONUS) region, to keep the analysis tractable and because
118 CONUS has detailed information on yearly crop production and water use.

119 CONUS is a major producer and contributor to the global production of three primary crops:
120 maize, soybean, and wheat. These crops were selected due to their substantial impact on the
121 agricultural landscape and their pivotal role in shaping global food production trends. The
122 CONUS serves as an ideal study area owing to its extensive availability of relevant data,
123 particularly on agricultural statistics and irrigation water withdrawals, which can provide a
124 basis for analysis and model evaluation. Additionally, the CONUS region exhibits diverse
125 climatic and geographic conditions, contributing to a better understanding of crop and water
126 system dynamics and their responses to various environmental factors.

127 To this end, we developed a coupled global hydrological-crop growth model framework to
128 investigate the intricate feedback between water availability and crop growth, focusing on three
129 key scientific objectives: ~~answer questions related to~~ 1) assessing the impacts of irrigation and
130 hydrology on crop growth; 2) investigating the feedbacks of crop growth on the hydrological
131 system when accounting for interannual variability; and 3) evaluating the importance of the
132 two-way coupling between hydrology and crop growth to provide realistic water resources and
133 crop yield simulations. By delving into these aspects, we aim to contribute valuable insights

134 into the feedback processes between hydrology and crop growth, thereby addressing the current
135 research gap in a more comprehensive manner.

136 The rationale behind coupling the hydrological and crop growth models lies in the need to
137 accurately capture the dynamic interactions between these systems, ensuring that both the water
138 availability and crop growth are represented with a sufficient level of sophistication in the
139 simulations to understand crop-water interactions. The coupling allows for the exchange of
140 critical variables such as soil moisture, evapotranspiration, and crop water uptake, which are
141 essential for understanding and predicting the impacts of environmental changes on agricultural
142 productivity and water resources. The justification for this coupling, including its expected
143 benefits and the technical approach, is detailed in section 2.2.

144 We hypothesize that the feedback between hydrology and crop growth is significant and
145 complex. Changes in soil moisture and water availability are expected to directly influence
146 crop water uptake, growth rates, and yield outcomes. Conversely, crop processes such as
147 evapotranspiration and root water uptake are likely to impact soil moisture levels, groundwater
148 recharge, and surface water flows, thereby altering water resources. Furthermore, we anticipate
149 that the integration of real-time crop data into hydrological models will enhance the accuracy
150 of predictions regarding water stress, irrigation needs, and crop productivity.

151 To address this, the PCR-GLOBWB 2 hydrological model (Sutanudjaja et al., 2018) is coupled
152 to the WOFOST crop model (de Wit et al., 2019) at a daily timestep and at a 5--arc minutes
153 (~10 km) spatial resolution applied to CONUS (section 2.1). In examining the interaction
154 between hydrology and crop growth, we consider both one-way and two-way interactions.
155 First, a one-way coupling is established to evaluate the effect of the simulated water availability
156 of PCR-GLOBWB 2 for rainfed and irrigated crop growth in WOFOST (section 2.1; section
157 2.32.1). In addition, a two-way coupling is established in which, additional to passing water
158 availability from PCR-GLOBWB 2 to WOFOST, the crop phenology of WOFOST in terms of
159 actual evapotranspiration, leaf area index and rooting depth is fed back into PCR-GLOBWB 2
160 (section 2.1, 2.32.2);).

161 ~~Furthermore, our framework was tested by comparing~~ individual WOFOST and coupled one-
162 way and two-way model runs ~~were compared~~ to evaluate the impacts of ~~feedbacks~~ feedbacks
163 on crop yield and irrigation water use (section 2.34). The results of these simulations are
164 compared with and evaluated against reported yield statistics and reported annual irrigation
165 withdrawals to assess their validity (section 2.45; section 3). In the end, we elaborate on the

166 uncertainties, strengths, and usability of our coupled model framework for studying the water-
167 food nexus under global change (section 4).

168

169 2 Methods

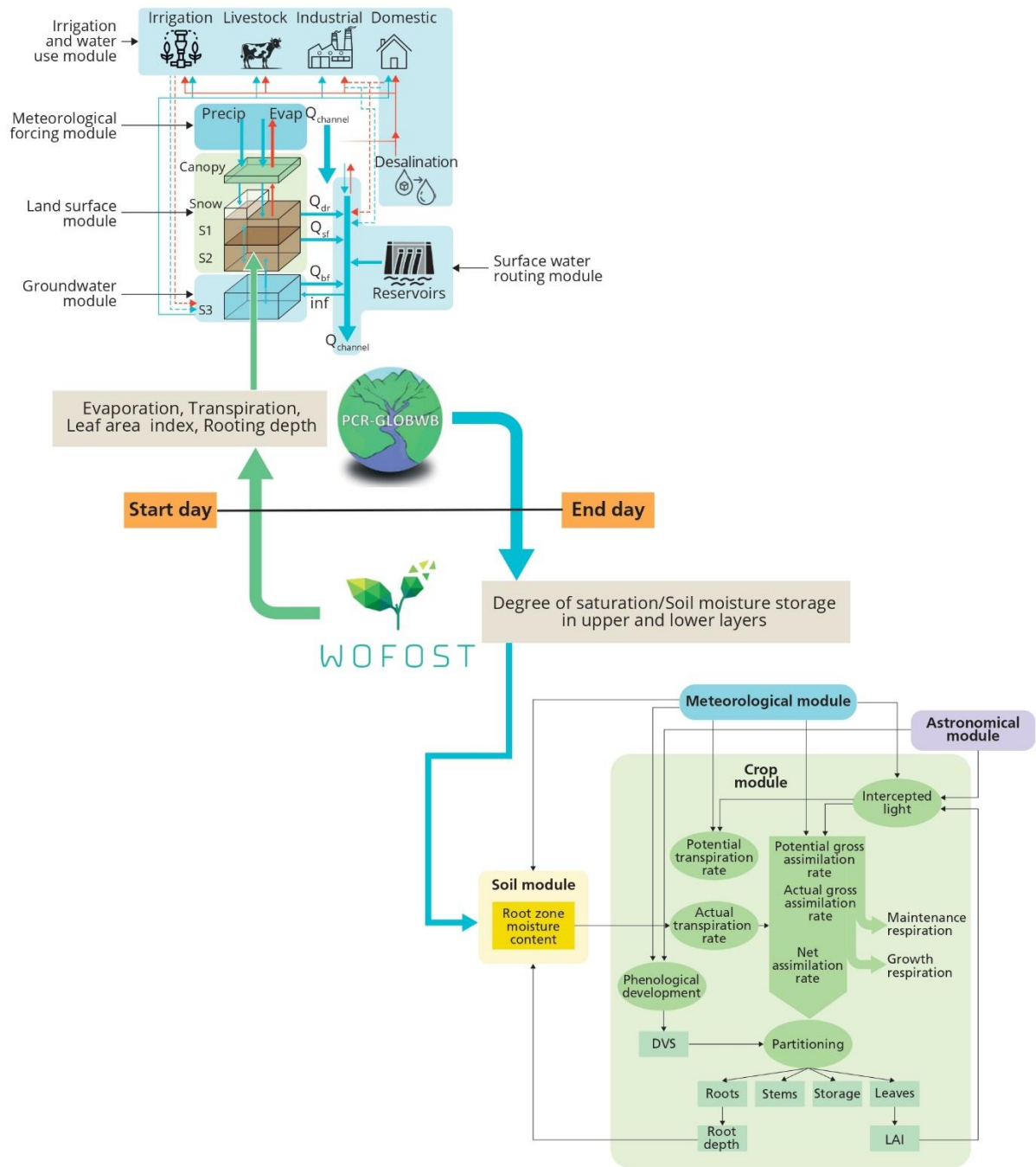
170 ~~Coupled PCR-GLOBWB 2-WOFOST model framework~~

171 ~~A new fully coupled PCR-GLOBWB 2-WOFOST model framework is developed to include~~
172 ~~the feedbacks between crop growth and hydrology. Here, we included both a one-way and two-~~
173 ~~way coupling between the PCR-GLOBWB 2 global hydrology and water resources model~~
174 ~~(Sutanudjaja et al., 2018) and the WOFOST crop growth model (de Wit et al., 2019). This~~
175 ~~coupled framework was then used to quantify the impacts of included feedbacks between~~
176 ~~hydrology and crop growth on a daily timestep and 5 arcminutes resolution for CONUS. The~~
177 ~~following (sub)sections provide a description of the PCR-GLOBWB 2 and WOFOST models~~
178 ~~and modules used (2.1), the model coupling setup (2.2), model coupling simulation~~
179 ~~experiments and parametrization (2.3), validation of crop yield and of irrigation water use (2.4).~~

180 A newly coupled hydrological-crop model framework (Fig. 1) is developed to include the
181 feedback between crop growth and hydrology. Here, we chose WOFOST as the crop growth
182 model because of its detailed crop phenology and development and PCR-GLOBWB 2 as the
183 hydrological model because of its detailed hydrological process simulation and large-scale
184 applicability. This framework includes both a one-way and two-way coupling between the
185 PCR-GLOBWB 2 global hydrological and water resources model (Sutanudjaja et al., 2018)
186 and the WOFOST crop growth model (de Wit et al., 2019). The coupled framework was then
187 used to quantify the impacts of included feedbacks between hydrology and crop growth on a
188 daily timestep and 5 arcminutes resolution for CONUS.

189 The following (sub)sections provide a description of the PCR-GLOBWB 2 and WOFOST
190 models and modules used (2.1), justification of coupling (2.2), the model coupling setup (2.3),
191 model coupling simulation experiments and parametrization (2.3), validation of crop yield and
192 of irrigation water use (2.4).

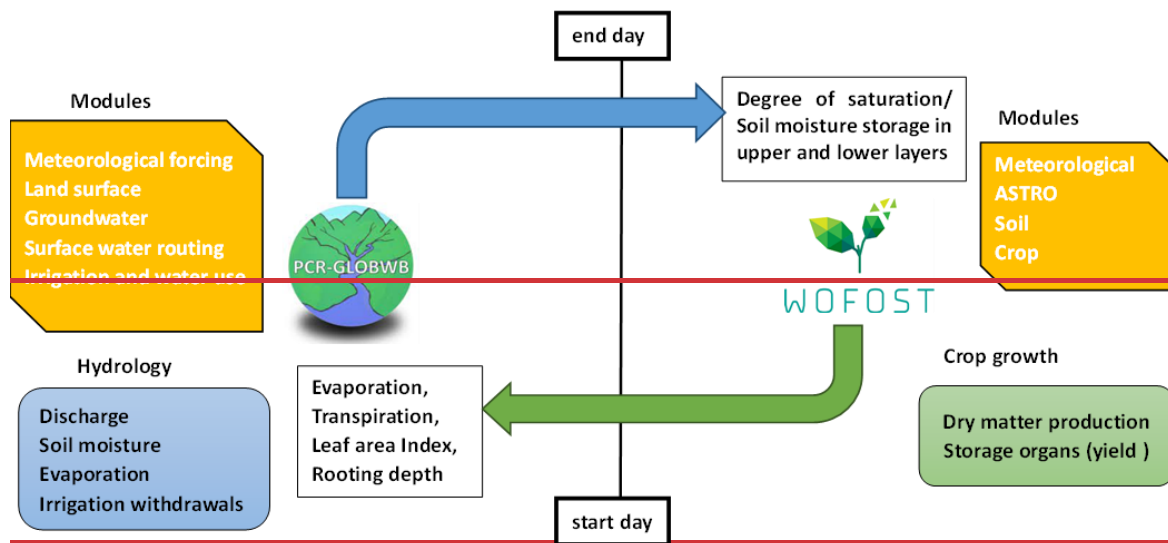
193



194

195 **Figure 1: The coupled model framework of the PCR-GLOBWB 2 hydrological and water**
 196 **resource model and the WOFOST crop growth model along with their model structures. The blue**
 197 **arrow represents the one-way coupling from PCR-GLOBWB 2 to WOFOST and the variables**
 198 **that are exchanged; the green arrow is added in case the full two-way coupling is considered. At**
 199 **the start of the day, WOFOST computes evapotranspiration, leaf area index, and rooting depth**
 200 **that is used by PCR-GLOBWB 2 to compute soil moisture status. At the end of the day, soil**
 201 **moisture storage in the upper and lower layers from PCR-GLOBWB 2 is fed to WOFOST to**
 202 **compute crop growth for the next day.**

203



204

205 **Figure 1: The coupled model framework of the PCR-GLOBWB 2 hydrology and water resources model**
 206 **and the WOFOST crop growth model. The blue arrow represents the one-way coupling from PCR-**
 207 **GLOBWB 2 to WOFOST and the variables that are exchanged; the green arrow is added in case the full**
 208 **two-way coupling is considered. At the start of the day, WOFOST computes evapotranspiration, leaf area**
 209 **index, and rooting depth that is used by PCR-GLOBWB 2 to compute soil moisture status. At the end of**
 210 **the day, soil moisture storage in the upper and lower layers from PCR-GLOBWB 2 is fed to WOFOST to**
 211 **compute crop growth for the next day.**

212

213 **2.1. Model description**

214 **PCR-GLOBWB 2**

215 The PCRaster Global Water Balance (PCR-GLOBWB 2) model (Sutanudjaja et al., 2018) is a
 216 global hydrology and water resource model developed at Utrecht University. This model
 217 operates on a latitude-longitude grid for which it simulates fluxes and stores of the terrestrial
 218 hydrological cycle with a daily resolution and dynamically includes anthropogenic impacts
 219 such as man-made reservoirs and sectoral water demands, water withdrawals, consumptive
 220 water use, and return flows. The PCR-GLOBWB 2 model currently consists of five main
 221 hydrological modules encompassing meteorological forcing, land surface, groundwater,
 222 surface water, irrigation and water use (Fig. 1).

223 The PCRaster Global Water Balance (PCR-GLOBWB 2) model (Sutanudjaja et al., 2018),
 224 developed at Utrecht University, is a global hydrological and water resource model that
 225 operates on a latitude-longitude grid. This model simulates the terrestrial hydrological cycle
 226 with daily resolution, incorporating anthropogenic impacts like man-made reservoirs, sectoral
 227 water demands, withdrawals, consumptive use, and return flows. PCR-GLOBWB 2 is applied
 228 and tested across local to global scales.

229 PCR-GLOBWB 2 utilizes time-explicit schemes for all dynamic processes, running on daily
230 time steps for hydrology and water use, and sub-daily steps for hydrodynamic river routing. It
231 simulates moisture storage in two upper soil layers and manages water exchange among the
232 soil, atmosphere, and groundwater. Atmospheric interactions include precipitation,
233 evaporation, transpiration, and snow processes. The model considers sub-grid variability in
234 land use, soils, and topography, influencing run-off, interflow, groundwater recharge, and
235 capillary rise. Run-off is routed through river networks using methods ranging from simple
236 accumulation to kinematic wave routing, supporting floodplain inundation and surface water
237 temperature simulation.

238 The model includes a reservoir operation scheme for over 6000 human-made reservoirs from
239 the GRanD database, integrated according to their construction year. Human water use is
240 comprehensively modeled, estimating sectoral water demands and converting them into
241 withdrawals from groundwater, surface water, and desalination sources, while accounting for
242 resource availability and groundwater pumping capacity. Consumptive use and return flows
243 are calculated for each sector.

244 ~~The PCR-GLOBWB 2 meteorological forcing uses a gridded time series of temperature and~~
245 ~~precipitation as input. More information on input datasets is provided in supplementary I.~~
246 ~~Reference potential evaporation is computed within the model using Hamon's (1963) method.~~
247 ~~The resulting reference potential evaporation is then employed in the land surface module to~~
248 ~~calculate the crop-specific land cover potential evaporation. Separate soil conditions are~~
249 ~~specified for each land cover type, with vegetative and soil properties varying accordingly for~~
250 ~~each grid cell and land cover type. The groundwater and surface water modules simulate the~~
251 ~~fluxes and stores of groundwater and surface water, respectively. The irrigation and water use~~
252 ~~module focuses on simulating water demand, withdrawals, consumption, and return flows. For~~
253 ~~a more detailed understanding of each module, we refer to the comprehensive description~~
254 ~~provided by Sutanudjaja et al. (2018).~~

255 PCR-GLOBWB 2's flexible structure encompasses five main hydrological modules:
256 meteorological forcing, land surface, groundwater, surface water, irrigation, and water use. The
257 meteorological module uses gridded temperature and precipitation data. Reference potential
258 evaporation is calculated using Hamon's method and employed in the land surface module to
259 determine crop-specific potential evaporation. The groundwater and surface water modules
260 handle fluxes and stores for groundwater and surface water, respectively. The irrigation and

261 water use module simulates water demand, withdrawals, consumption, and return flows,
262 sourcing water from surface water (rivers and reservoirs), groundwater (both renewable and
263 non-renewable), and desalinated water, depending on availability. Detailed descriptions of
264 each module are provided by Sutanudjaja et al., (2018).

265 **WOFOST**

266 WOFOST (WOrld FOod STudies) is a crop simulation model developed at Wageningen
267 ‘School of De Wit’, in the Netherlands, designed to quantitatively analyze the crop growth and
268 potential production of annual field crops at the field scale (Supit et al., 1994). WOFOST
269 employs a fixed time step of one day to simulate crop growth based on eco-physiological
270 processes such as phenological development and growth (de Wit et al., 2019). WOFOST has
271 found extensive application in assessing the impacts of climate change and management
272 strategies on crop growth and yield at local to global scales (Droppers et al. 2021).

273 The WOFOST crop model comprises of four modules: meteorological, crop, astronomical and
274 soil weather, crop, astro and soil (Fig. 1). The WOFOST modules simulate a range of processes,
275 including phenological development, CO₂ assimilation, leaf development, light interception,
276 transpiration, respiration, root growth, assimilated partitioning to the various organs and the
277 formation of dry matter. The model’s output includes simulated crop biomass total, crop yield
278 and variables such as leaf area and crop water use.

279 Temperature effects on crop development within WOFOST are modeled using temperature
280 sums, which accumulate daily temperatures above a specified threshold. These sums influence
281 germination and phenological stages, thereby affecting CO₂ assimilation. Additionally, the
282 model accounts for the direct and indirect effects of suboptimal daytime temperatures on crop
283 growth and development, which are critical to overall plant performance. Daily photosynthesis
284 in the crop growth model is simulated by considering absorbed radiation and water stress. After
285 accounting for the assimilates used in maintenance respiration, the remaining resources are
286 allocated among the plant’s leaves, stems, roots, and storage organs. A key internal driver of
287 this process is the leaf area index (LAI), which results from leaf area dynamics governed by
288 photosynthesis, biomass allocation, leaf age, and developmental stage. LAI, in turn, influences
289 the daily rates of photosynthesis.

290 WOFOST has been finely tuned to account for diverse climate and soil conditions, particularly
291 for commonly studied crops such as maize, soybean, and wheat, thereby, reducing the need for
292 further recalibration. This pre-tuning ensures that simulations reliably capture the growth and

293 yield responses of these crops under varying environmental conditions. For more detailed
294 information on the fine-tuning of crop variables, see (de Wit & Boogaard, 2021).

295 WOFOST employs a classic water balance approach designed for freely draining soils where
296 groundwater is too deep to affect soil moisture content in the rooting zone. This approach
297 divides the soil profile into two compartments: the rooted zone and the lower zone extending
298 from the actual rooting depth to the maximum rooting depth. The subsoil below this maximum
299 rooting depth is not considered. As roots extend deeper towards the maximum rooting depth,
300 the lower zone gradually merges with the rooted zone. This approach is suitable for regional
301 applications with limited soil property information. Soil moisture in the root zone serves as a
302 primary link between the WOFOST model and the underlying soil module. For a detailed
303 description of the WOFOST crop growth model, we refer to (de Wit & Boogaard, (2021) and;
304 Supit et al., (1994).

305 **2.2. Justification of model coupling**

306 The integration of the hydrological model PCR-GLOBWB 2 (Sutanudjaja et al., 2018) with
307 the crop growth model WOFOST (Supit et al., 1994) is crucial for accurately simulating the
308 complex interactions between water availability and crop development. The hydrological
309 model PCR-GLOBWB 2 is designed to simulate hydrological processes such as river
310 discharge, groundwater flow, and water storage dynamics. It provides detailed representation
311 and insights into the state and dynamics of water resources over large spatial scales and long
312 temporal scales. On the other hand, the crop growth model WOFOST is focused on simulating
313 crop phenology, including the stages of crop development, growth, and yield formation under
314 varying environmental conditions.

315 Despite the strengths of each model, they individually have limitations that can affect the
316 accuracy of simulations. PCR-GLOBWB 2 relies on static vegetation parameters, such as fixed
317 Leaf Area Index (LAI) and root depth, which can limit its ability to reflect the dynamic nature
318 of crop growth. On the other hand, WOFOST offers a detailed and dynamic representation of
319 crop phenology and development, adjusting parameters like LAI and root depth based on actual
320 growth stages. However, WOFOST employs a simplified water balance model, that may not
321 adequately capture complex hydrological interactions.

322 To address these limitations, it is important to combine the strengths of both models to enhance
323 hydrological and crop modelling performance. By integrating, WOFOST's detailed crop
324 growth simulation capabilities with the robust hydrological process simulations of PCR-

325 GLOBWB 2, we can better understand and represent the soil-plant-atmosphere interactions.
326 Therefore, this study integrates PCR-GLOBWB 2 and WOFOST by passing soil moisture data
327 from PCR-GLOBWB 2 to WOFOST and feeding vegetative fluxes from WOFOST back into
328 PCR-GLOBWB 2 on a daily basis. Additionally, to understand the intricate dynamics between
329 hydrology and crop model, PCR-GLOBWB 2 is coupled to the WOFOST in one-way and two-
330 way interactions.

331 In evaluating various coupling methods for integrating hydrological and crop models, we
332 identified several approaches, including one where the hydrological model directly provides
333 detailed irrigation schedules and percolation rates to the crop model. While this method offers
334 highly detailed hydrological inputs, it often leads to inconsistencies due to the separate
335 handling of soil moisture dynamics between the models, resulting in errors in soil moisture
336 management and water balance. Commonly used coupling procedures, such as those described
337 by (Li et al., (2014) and (Tsarouchi et al., (2014), calculate potential evapotranspiration and
338 vegetation water uptake within the hydrological model, which is then passed to the crop model
339 to simulate crop growth. The crop model then calculates state variables like leaf area index,
340 root depth, and canopy height, which are subsequently fed back into the hydrological model.
341 However, these methods can introduce system errors, particularly in the transpiration module,
342 if there is a discrepancy between evapotranspiration calculated by the crop and hydrological
343 model, as highlighted by Wang et al., (2012). Our chosen coupling method, where soil moisture
344 is calculated by PCR-GLOBWB 2 and passed to WOFOST and vegetative dynamics and
345 evapotranspiration fluxes are then fed back into PCR-GLOBWB 2, offers a balanced approach
346 that ensures consistency, and the necessary complexity, and efficiency in the simulations.

347 The selected coupling approach also addresses specific challenges associated with the models.
348 PCR-GLOBWB 2 allows for flexible land cover classification and parameterization, which is
349 essential for accurately representing diverse crop types and their interactions with water
350 resources. For this study, we defined 12 land cover types (tall natural, short natural, pasture,
351 irrigated maize, irrigated soybean, irrigated wheat, non-paddy irrigated crops (irrigated other
352 crops), paddy irrigated crop, rainfed maize, rainfed soybean, rainfed wheat and rainfed others.
353 WOFOST's role in this coupling is to pass the fluxes of irrigated and rainfed maize, soybean
354 and wheat to PCR-GLOBWB 2, ensuring a detailed simulation of crop water use.

355 One of the key considerations in this coupling is accurately calculating the soil-water balance.
356 Given its more advanced soil moisture accounting scheme, PCR-GLOBWB 2 handles this

357 aspect, as WOFOST's simpler single-layer leaky bucket approach could introduce
358 complexities if soil moisture data were passed from WOFOST to the multi-layered soil model
359 of PCR-GLOBWB 2. Therefore, the coupling approach we selected minimizes potential
360 discrepancies while maximizing the strengths of each model.

361 It is important to acknowledge, that individual models come with inherent uncertainties, related
362 to model structure, parameters and data. When coupling these models, the level of uncertainty
363 compounds further (Kanda et al., 2018). Additionally, the nature of coupling itself can
364 introduce another layer of uncertainty. According to (Antle et al., (2001), coupling models lead
365 to further conceptualization and computational problems, elevating uncertainty levels.
366 Therefore, an efficient coupling is essential to minimize these risks. There are three primary
367 methods for coupling models (Vereecken et al., 2016): light/loose coupling,
368 external/framework coupling using a central coupler, and full coupling.

369 In light or loose coupling, the output of one model serves as the input for the other, which can
370 lead to a straightforward but limited interaction. Framework coupling uses a central coupler for
371 communication between models without requiring code modification, offering a balance
372 between integration and flexibility. Full coupling involves both models sharing the same
373 boundary conditions, drivers, and variables, which requires significant code modification.

374 **Implementation of the (BMI) framework coupling**

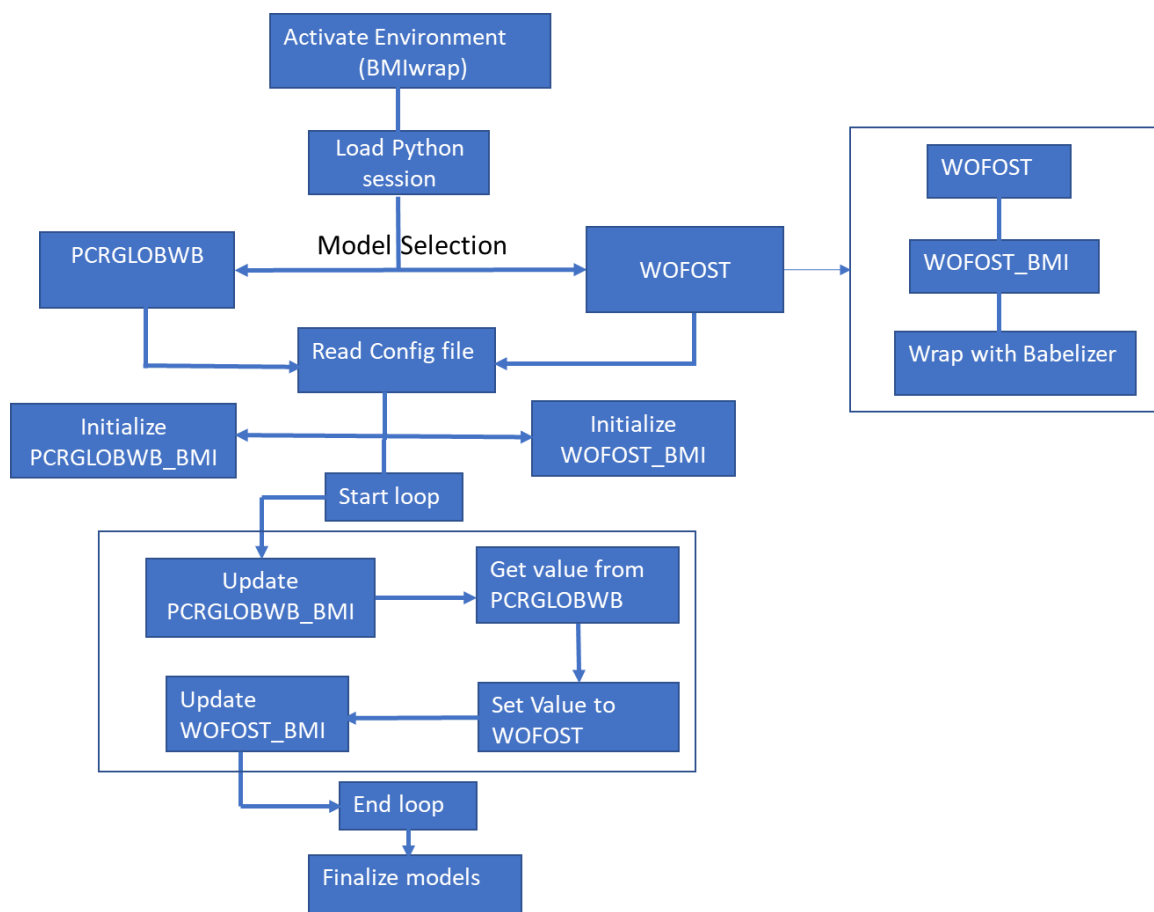
375 Given the complexity of integrating the PCR-GLOBWB 2 and WOFOST models and the need
376 for efficient simulations, we opted for framework coupling. This approach was chosen because
377 WOFOST and PCR-GLOBWB 2 are written in different programming languages (C and
378 PCRaster-Python, respectively). Framework coupling allows for seamless interaction between
379 the models at each time step, facilitating dynamic exchanges while limiting I/O-related
380 computation times. We employed the Basic Model Interface (BMI) for this purpose (Hutton et
381 al., 2020; Peckham et al., 2013). The decision to use BMI over alternative techniques was
382 driven by its non-interfering nature, ensuring no code entanglement and facilitating seamless
383 connection between the two models. BMI functions act as a bridge, enabling direct variable
384 exchange between WOFOST and PCR-GLOBWB 2 without modifying their source code. This
385 non-invasive approach ensures a flexible and robust coupling framework, allowing continuous
386 model development without interruptions. Integrating BMI functions into both models
387 provides a set of functions for retrieving or altering model variables, enhancing adaptability
388 and efficiency.

389 An additional wrapper was required to translate the model-specific BMI functions into Python-
 390 compatible information to establish a Python-based coupling framework. The Babelizer
 391 wrapper (CSDMS, 2024) was utilized for this purpose with the WOFOST BMI. Conversely,
 392 no supplementary wrapper is needed in the PCR-GLOBWB 2 BMI, as the model is inherently
 393 Python-compatible due to its programming language.

394 The Babelizer wrapper facilitates the integration of the WOFOST model by utilizing an input
 395 file that provides essential details, including the model library, entry point, packages, and
 396 author information. This input file guides the construction of the necessary dependencies to
 397 generate Python bindings. Once these Python bindings are created, Babelizer ensures the
 398 successful integration of the WOFOST BMI into Python by verifying that the bindings are
 399 correctly built and loaded.

400 **Workflow of PCR-GLOBWB 2 - WOFOST model framework**

401 In the PCR-GLOBWB 2 - WOFOST coupling framework, the workflow after implementing
 402 BMI functions remains consistent for both one-way and two-way coupling, up until the
 403 initialization of the hydrological and crop models (Fig. 2).



404

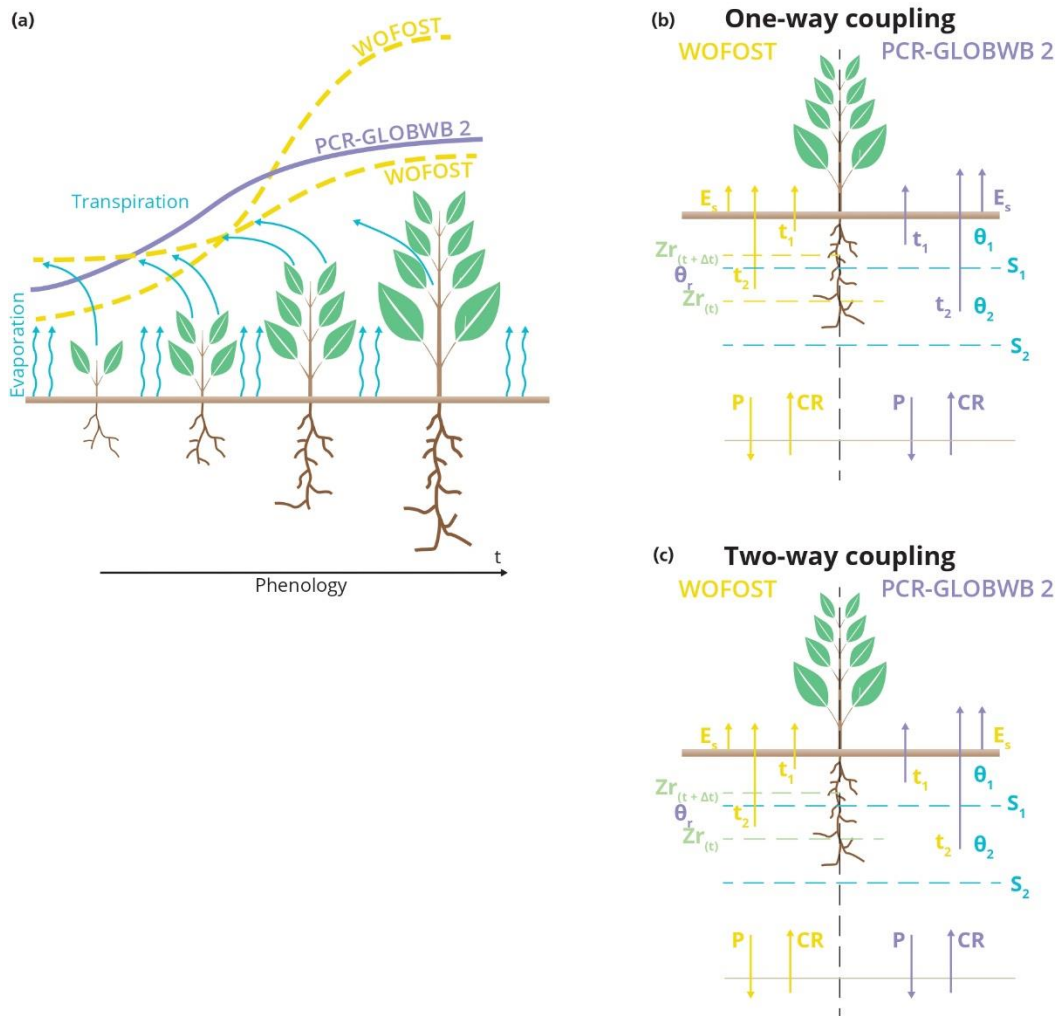
405 **Figure 2: Schematization of the workflow of the coupled PCR-GLOBWB 2 - WOFOST**
406 **model framework**

407 Before initiating the Python session, it is crucial to activate the BMI wrap environment, which
408 includes all necessary libraries for both hydrological and crop models. After this setup, the
409 PCR-GLOBWB 2 and WOFOST models, along with their configuration files that define the
410 coupling settings, are loaded into the Python session. BMIwrap reads the configuration file,
411 initializing the model-specific configuration settings before establishing both models as a
412 coupled entity.

413 Once the coupled models are initialized, a loop is initiated, commencing at the start time and
414 concluding at the end time. During each iteration of this loop, variables are exchanged between
415 the models based on the one-way or two-way coupling configuration. This iterative process
416 ensures a continuous and seamless flow of information between the PCR-GLOBWB 2
417 hydrological model and the WOFOST crop model throughout the simulation period.

418 **2.3.Model coupling setup**

419 The developed PCR-GLOBWB 2 - WOFOST coupled model framework integrates
420 hydrological and crop models through both one-way and two-way couplings, as illustrated in
421 Fig. 1 & 3. This model coupling aims to assess the intricate interactions between hydrology and
422 crop growth under different agricultural conditions, specifically irrigated and rainfed settings.
423 The one-way coupling examines the impact of water availability on crop growth, while the
424 two-way coupling incorporates the exchange of soil moisture status and hydrological
425 parameters and fluxes based on crop status.



426

427 Figure 3: Schematic view of the coupled model framework: a) shows the calculated phenology
 428 from WOFOST and PCR-GLOBWB 2 over time along with the associated fluxes. b) displays
 429 a detailed representation of the one-way coupling approach, where variables such as soil
 430 moisture are exchanged from PCR-GLOBWB 2 to WOFOST and (c) illustrates the two-way
 431 coupling approach, where variables are exchanged in both directions between PCR-GLOBWB
 432 2 and WOFOST.

433 2.3.1. One-way coupling

434 In the one-way coupling, information on soil hydrology-moisture status is passed from PCR-
 435 GLOBWB 2 to WOFOST (Fig 43(b)). Here, PCR-GLOBWB 2 simulates soil moisture content
 436 for every day and the soil water storage is simulated separately for each land cover type.
 437 Consequently, WOFOST receives the soil moisture content from PCR-GLOBWB 2 as input,
 438 with generally higher values of soil moisture for irrigated crops than of nearby rainfed crops.

439 WOFOST then simulates the crop yield based on the simulated soil moisture content and the
440 same meteorological inputs as PCR-GLOBWB 2 uses.

441 The combined model framework captures the impact of hydroclimatic conditions by assessing
442 water stress and heat stress. Water stress, influenced by soil moisture levels derived from PCR-
443 GLOBWB 2, affects various processes in WOFOST such as a reduction in the leaf area, a
444 decrease in the assimilation of biomass (growth), changes in the partitioning of biomass, and
445 an increase in various plant organs of senescence (ageing processes). Elevated temperatures
446 have varying effects across different stages of crop development. They can accelerate crop
447 growth by promoting faster accumulation of Growing Degree Days, which are essential for
448 determining crop maturity. However, prolonged exposure to high temperatures can also induce
449 heat stress, adversely impacting crop health and potentially shortening the overall duration of
450 the crop's growth cycle. Insufficient water availability that limits the evapotranspiration also
451 reduces the amount of assimilation and the corresponding yield.

452 **2.3.2. Two-way coupling**

453 In addition to one-way coupling, the two-way coupling approach involves iterating data
454 exchange between WOFOST and PCR-GLOBWB 2 twice per day. WOFOST calculates the
455 vegetation states, (such as leaf area index (LAI), biomass and root depth) and fluxes (e.g.
456 evapotranspiration) for irrigated and rainfed maize, soybean and wheat crops, while other
457 vegetation and non-vegetation fluxes for other crops are simulated within PCR-GLOBWB 2.
458 To be more specific, for the fraction of land cover that is different from maize, wheat and
459 soybean, the vegetation states and fluxes are calculated within the PCR-GLOBWB 2. For these
460 land cover types, vegetation phenology in the form of crop factors, is approximated by a yearly
461 climatology. ~~vegetation-related states and fluxes are passed from WOFOST to PCR-GLOBWB~~
462 ~~2 and data exchange between the two models is iterated twice per day.~~ In the two-way coupling,
463 information data is exchanged between PCR-GLOBWB 2 and WOFOST as follows (Fig. 43c):

- 464 • At the start of the day, PCR-GLOBWB 2 passes the previous day's soil moisture to the
465 WOFOST, assuming no root development has occurred overnight. -WOFOST then
466 computes the potential evapotranspiration ~~on the basis~~based on-~~of~~ the meteorological
467 variables at the current time step and the pertinent vegetation states from the previous
468 time step (leaf area index (LAI), rooting depth, and crop height). ~~It also calculates, as~~
469 ~~well as~~ the actual bare soil evaporation, actual transpiration (actual evapotranspiration),
470 potential evaporation and ~~the~~ open water evaporation;

- 471 • The calculated fluxes are passed to PCR-GLOBWB 2, together with the root depth. The
472 root depth is used to partition the actual transpiration from the single root zone of
473 WOFOST over the two soil layers of PCR-GLOBWB 2, dependent on the root content.
474 For both irrigated and rainfed crops, the actual evapotranspiration from WOFOST is
475 ~~imposed forced to~~ PCR-GLOBWB 2 and used to update the soil moisture content of
476 the two soil layers in PCR-GLOBWB 2 for the current daily timestep;
- 477 • In the case of irrigated crops, the stages of vegetated development are used to compute
478 the amount of irrigation in PCR-GLOBWB 2. Potential evaporation is used to calculate
479 the irrigation water demand for paddy crops (not considered here), whereas the
480 irrigation water requirement for non-paddy crops is computed based on ~~on the basis of~~
481 the soil moisture status according to the FAO guidelines (Allen et al., 1998). The
482 irrigation water requirement is withdrawn from the available water resources in PCR-
483 GLOBWB 2 and the available irrigation water supply is applied to the crops in addition
484 to any natural precipitation;
- 485 • At the end of the day, ~~The~~ the resulting soil moisture ~~from~~ of the two soil layers from PCR-
486 GLOBWB 2 is aggregated to provide a total ~~the average value~~ for the root zone of each
487 crop, which is then ~~and~~ passed back to WOFOST;
- 488 • Using the updated ~~With the~~ soil moisture from PCR-GLOBWB 2, WOFOST computes
489 the actual transpiration and updates ~~the~~ crop growth and the crop status. ~~is updated.~~ The
490 new fluxes and ~~new~~ crop parameters are then passed to PCR-GLOBWB 2 again on the
491 next day in the next daily timestep (Fig. 1, Fig. 3c).

492 In this two-way coupling, the crop phenology from WOFOST determines evapotranspiration
493 and thus the soil hydrology of PCR-GLOBWB 2, particularly during dry spells. Compared to
494 the predefined phenology of PCR-GLOBWB 2, the LAI, rooting depth and evapotranspiration
495 as simulated by WOFOST will lag during dry spells and less water may be lost from PCR-
496 GLOBWB 2. However, the thinner rooting depth will also lead to an earlier drying out of the
497 soil and reduced capillary rise. This subsequently leads to reduced soil moisture (compared to
498 PCR-GLOBWB 2 standalone) which in turn feeds back to a reduced simulated yield in
499 WOFOST, in particular for rainfed crops. For irrigated crops, the extra water supplied will
500 largely offset these feedbacks and result in near-optimum growth.

501 **2.4. Model coupling simulation experiments and parametrization**

502 Hydrological simulations were conducted with a daily timestep at a 5-arcminute grid
503 resolution, where for each grid cell WOFOST was used to simulate crop growth for irrigated
504 and rainfed maize, soybean, and wheat. To assess the impact of hydrology on crop growth and
505 understand the interactions between hydrology and crop growth, three sets of simulations were
506 carried out for both irrigated and rainfed crops: a) standalone simulations using the WOFOST
507 crop model solely, b) one-way coupled, and c) two-way coupled PCR-GLOBWB 2 - WOFOST
508 simulations. Note that for the standalone simulations with WOFOST under irrigation the
509 potential crop yield is simulated, which is potential yield without water (and nutrient) stress
510 except for temperature effects. When coupled to PCR-GLOBWB 2, water stress can occur even
511 for irrigated crops in case there is not enough water available (in PCR-GLOBWB 2) to fully
512 satisfy the crop water demand. For rainfed crops, growth is influenced by available soil
513 moisture for all simulations and is thus sensitive to water stress and temperature. Green water
514 from natural rainfall is the primary water supply in rainfed analysis, while irrigated crops get
515 water from both green and blue water (from surface water and renewable groundwater) and
516 non-renewable groundwater leading to groundwater depletion.

517 Daily timestep simulations covered the period from 1979 and 2019, using weather variables
518 (minimum and maximum air temperature, short wave radiation, precipitation, vapour pressure,
519 windspeed, and humidity) from the W5E5 forcing data (Lange et al., 2021) as input to PCR-
520 GLOBWB 2 (Sutanudjaja et al., 2018) and WOFOST. Cropland areas and growing seasons
521 were determined from the MIRCA2000 (Portmann et al., 2010) global monthly irrigated and
522 rainfed crop area dataset. The focus of the coupled framework was to comprehend the impacts
523 and feedback between hydrology and crop growth. Crop parameters, atmospheric CO₂
524 concentrations, and fertilizer application were obtained from the WOFOST crop parameter
525 dataset for each crop (WOFOST Crop Parameters, 2024). Cultivars in the WOFOST crop
526 parameter datasets were calibrated for each crop against reported agricultural yields from the
527 United States Department of Agriculture (USDA) National Agricultural Statistics Service
528 (USDA, 2024), with the closest matching cultivar selected for final simulations. Detailed
529 information on the cultivar calibration for each crop (i.e. irrigated and rainfed maize, soybean
530 and wheat) is provided in the supplementary information section III.

531 Comparisons were made between simulations from standalone WOFOST and the one-way and
532 two-way coupled PCR-GLOBWB 2 - WOFOST runs. This comparative analysis involved
533 evaluating the results from different model runs for crop growth against reported crop yields.

534 Furthermore, irrigation water withdrawals of coupled model runs are compared against the
535 USGS Water Use Database (USGS, 2023) (section 2.4).

536 **2.5.Model evaluation**

537 We evaluated the three different model configurations by comparing simulated results against
538 reported USDA crop yields of maize, soybean and wheat. Furthermore, we cross-referenced
539 our simulations with irrigation water withdrawal data spanning five years from the USGS
540 Water Use Database. Specifically, we compared data for the years 2005, 2010, and 2015, as
541 the USGS census data is collected at five-yearly intervals.

542 **2.5.1. Crop yields model evaluation**

543 To assess the model's performance, we employ three key metrics: correlation coefficients (r),
544 Normalized Root Mean Square Error (NRMSE) and Normalized Bias (NBIAS). These metrics
545 were selected for their ability to capture the strength, accuracy and systematic errors in the
546 relationship between simulated and observed values.

$$547 \quad r = \frac{\sum(P_i - \bar{P})(O_i - \bar{O})}{\sqrt{\sum(P_i - \bar{P})^2 \cdot \sum(O_i - \bar{O})^2}} \quad (1)$$

$$548 \quad NRMSE = \frac{\sqrt{\frac{1}{n} \sum_{i=1}^n (P_i - O_i)^2}}{\bar{O}} \quad (2)$$

$$549 \quad NBIAS = \frac{\frac{1}{n} \sum_{i=1}^n (P_i - O_i)^2}{\bar{O}} \quad (3)$$

550 Where, P_i and O_i are the individual predicted and observed values, respectively and \bar{P} and \bar{O}
551 are the means of the predicted and observed values.

552 The evaluation was done both temporally for average CONUS yields per year, as well as for
553 multi-year averages per state-per-state to evaluate the model's ability to capture spatial
554 variations in crop yield. This was done for both irrigated and rainfed maize, soybean and wheat.

555 To further characterize the dataset and evaluate the impact of the degree of coupling on
556 simulated yields, additional statistical analyses were conducted on the 41 years of simulated
557 data at the 5-arcminute grid scale. To this end, the mean and coefficient of variation (CV) were
558 computed for both one-way and two-way datasets for the three crops under irrigated and rainfed
559 conditions. The purpose of this analysis was to examine the central tendency and year-to-year
560 variability of yield simulations and how these are related to the way hydrology and crop growth
561 are coupled.

562 2.5.2. Irrigation water use model evaluation

563 The USGS reported irrigation water use data provides a comprehensive representation of the
564 total irrigation water utilized by all crops for a number of states (USGS, 2023). The irrigated
565 crop area used in this dataset is however not the same as that used in PCR-GLOBWB 2 which
566 is based on MIRCA2000 (Portmann et al., 2010). Thus, directly comparing USGS data with
567 our simulated water withdrawals would result in bias. To ensure a fair comparison between the
568 simulated and reported data for all crops, we adjusted the USGS irrigation water use data by
569 multiplying these with the ratio of the irrigated area from MIRCA2000 to the reported total
570 USGS irrigated area. Additionally, our simulated irrigation water withdrawal volumes did not
571 yet account for irrigation efficiency. We intend to implement this in future development.
572 Hence, we introduced an additional correction by dividing the simulated withdrawal data by
573 the irrigation efficiency as is commonly used in PCR-GLOBWB 2 when it is not coupled to a
574 crop model.

575 After these corrections, the coupled model simulated irrigation water withdrawals for all crops
576 were evaluated against actual irrigation data obtained from the USGS database through spatial
577 (multi-year averages per state) and temporal (multi-state totals per year) analysis, providing
578 insights into the model's ability to replicate observed irrigation water use patterns.

579 This comparison was limited to the years with available reported area data for the simulation
580 period (2005, 2010, 2015) and to the states with reported irrigation water withdrawal volumes
581 for these years (37 states).

582 3. Results

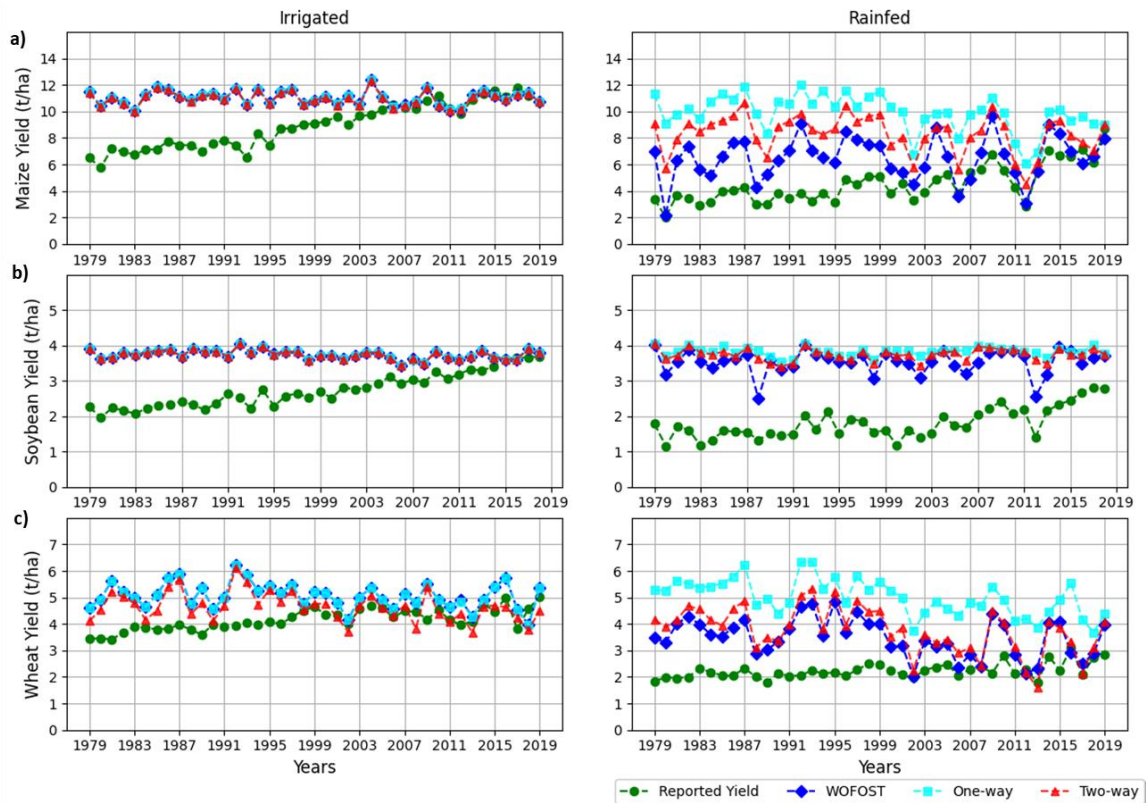
583 In this section, we present the key findings obtained from the implementation of the coupled
584 hydrological-crop growth model framework based on WOFOST and PCR-GLOBWB 2. We
585 present our findings sequentially, first delving into observed hydrological impacts on crop
586 growth (one-way coupling) and then exploring how feedback mechanisms between crop
587 growth and hydrology impact the crop growth system (two-way coupling).

588 3.1 Comparative temporal and spatial analysis of stand-alone, one-way, and two-way 589 coupling for irrigated and rainfed crops

590 Temporal analysis (Fig. 2) compares the simulated yields with reported yields for irrigated and
591 rainfed maize, soybean, and wheat crops spanning from 1979 to 2019 in the CONUS region.
592 Notably, the reported yields exhibit discernible trends for the CONUS region across the three

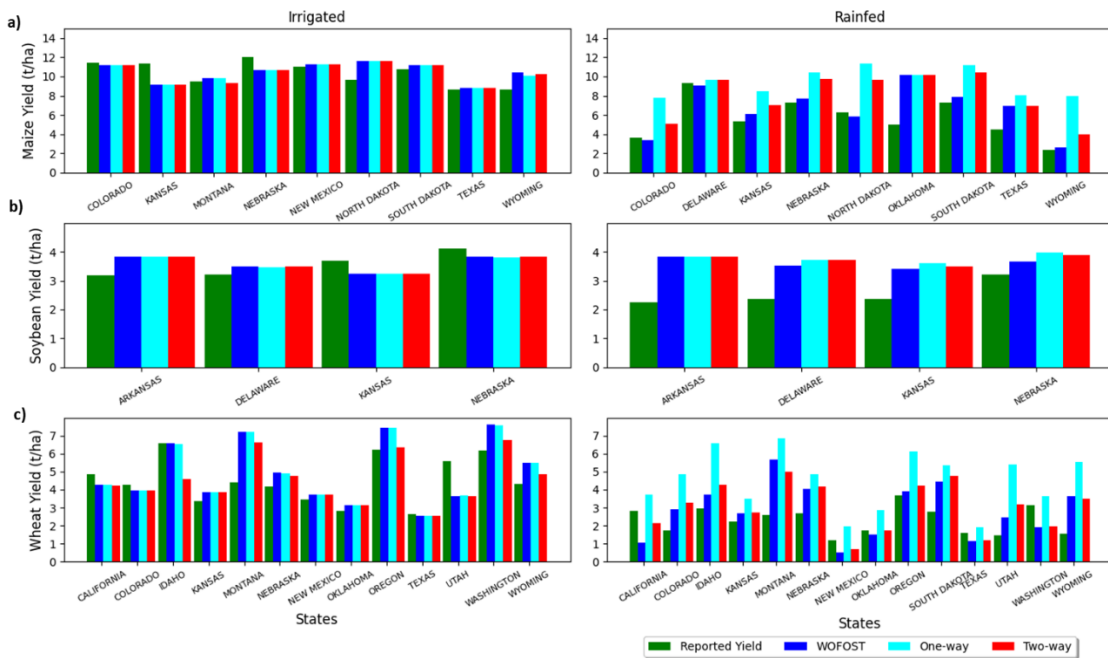
593 crops and in both irrigated and rainfed analysis. This temporal evolution is primarily attributed
594 to technological advancements, encompassing improved agricultural practices and the
595 introduction of enhanced crop varieties over the study period (Arata et al., 2020). In contrast,
596 simulated yields of our coupled PCR-GLOBWB 2 – WOFOST model framework ~~simulated~~
597 ~~yields~~ do not capture such trends, as the modelling approach intentionally omitted to
598 incorporate trends in technology and management practices. This intentional omission was to
599 focus on the intrinsic biophysical processes and climatic conditions affecting crop yields,
600 providing a baseline understanding unaffected by external advancements.

601 The trends in reported yields differ significantly across all crops and between irrigated and
602 rainfed systems. For maize, both irrigated and rainfed yields show an increasing trend,
603 particularly post-2000, which is not reflected in the simulated yields. Soybean yields exhibit a
604 gradual upward trend in irrigated systems, while rainfed soybean yields show little to no
605 discernible trend until 2007, followed by a slight increase. Wheat yields, both irrigated and
606 rainfed, demonstrate fluctuations with a slight upward trend towards the end of the period.
607 These discrepancies can be attributed to various factors, including technological advancements,
608 improved agricultural practices, and the introduction of enhanced crop varieties, which were
609 not incorporated into the modelling approach. To ensure a consistent and meaningful analysis,
610 we selected the years 2006-2019 for further analysis (spatial analysis (Fig. 5) and evaluation
611 metrics (Table. 1)). This period was selected because reported yields during these years appear
612 more stable and are better aligned with the simulated yields, allowing for a fair evaluation of
613 the model's accuracy and reliability. For the selected periods, we think that the results are
614 convincing, and, except for rainfed, Soybean, they are certainly up to par with the results from
615 other crop growth modelling studies at continental scales. For a consistent analysis, we
616 specifically focused on the years when reported yields appear to be more or less stable and in
617 line with our simulated yields. Consequently, the timeframe from 2006 to 2019 was selected
618 for further analysis. -



619

620 **Figure 42:** Temporal analysis of irrigated and rainfed crops of a) maize, b) soybean and c) wheat for the
 621 years 1979 to 2019 of a CONUS region



622

623 **Figure 53:** Spatial (i.e. state level) analysis of irrigated and rainfed crops of a) maize, b) soybean and c)
 624 wheat for the years 2006 to 2019 for the CONUS region.

625 Figures 42 and 35 show the outcomes of comparing simulated irrigated and rainfed analyses
 626 yields for maize, soybean, and wheat with reported yields. For the irrigated crops, the obtained

627 yields by standalone WOFOST represent the potential productivity for the three crops. Notably,
628 one-way, and two-way model runs for irrigated crops yielded nearly identical results to the
629 standalone runs, indicating that there is generally enough irrigation water to completely satisfy
630 crop water demands. This similarity arises because in irrigated conditions, water supply is
631 managed to meet crop water demands fully, thereby minimizing the influence of soil moisture
632 variability on yield outcomes. In other words, since the primary constraint, water availability
633 is alleviated by irrigation, the simulations naturally converge, regardless of the model coupling
634 approach. Although not shown here, we note that this is at the expense of non-renewable
635 groundwater use in states overlying the Southern Great Plains aquifer system.

636 Conversely, for rainfed crops, that rely solely on rainfall, we generally expect similar yields
637 from stand-alone and two-way coupled simulations, since the primary water input, is rainfall.
638 However, differences were observed between these models, especially more pronounced in
639 maize crops and less significant in soybean and wheat. These variations between the two
640 models can be attributed to various factors. The coupled model incorporates detailed soil
641 moisture dynamics, including processes like infiltration, percolation, and runoff, which directly
642 influence water availability for crops. For example, higher infiltration rates can increase soil
643 moisture, thereby increasing water available to crops, whereas greater percolation rates might
644 lead to water loss beyond the root zone, reducing available moisture. In contrast, standalone
645 WOFOST cannot accurately capture such variability, leading to differences in simulated yields.
646 Additionally, the coupled model integrates simulations of surface runoff and lateral water
647 redistribution, which impact local soil moisture levels. In areas with significant runoff, less
648 water infiltrates the soil, thereby reducing moisture availability for crops. This aspect is often
649 simplified or omitted in standalone crop models, which might assume uniform water
650 availability from rainfall. These differences contribute to the differences in simulated yields,
651 with the coupled model providing a more comprehensive simulation of hydrological conditions
652 affecting crop productivity.

653 ~~simulations produced comparable results, while the~~The one-way coupling approach tended to
654 exhibit an overestimation of yields relative to stand-alone and two-way simulations,
655 particularly for wheat and to a lesser degree for maize. This discrepancy arises from the fact
656 that in one-way coupling soil moisture calculations in PCR-GLOBWB 2 under drought
657 conditions assume a full rooting depth development (the phenology is fixed) which could, as
658 described before, lead to an over-estimation of soil moisture availability that is then passed to
659 WOFOST, eventually leading to an overestimation of yield. In contrast, the two-way coupling

660 approach feeds back information about the lagging behind of crop development to PCR-
661 GLOBWB 2, and dynamically adjusts the root zone depth based on actual crop development
662 stages. As a result, the two-way coupling approach results in more realistic soil
663 moisture and crop yield simulations, by the two-way coupling.

664 ~~The analysis of temporal variations in simulated irrigated and rainfed maize crop yields shows~~
665 ~~distinct year to year fluctuations. Rainfed maize, in particular, exhibits a discernible pattern~~
666 ~~with certain years marked by notable peaks in yields, contrasting with others that experienced~~
667 ~~comparatively lower production, revealing sensitivity to varying environmental conditions.~~
668 ~~These variations are also observed in reported maize yields. Similar year to year patterns are~~
669 ~~found for simulated irrigated and rainfed wheat yields, but not so in observed yields.~~
670 ~~Apparently, sensitivity to water and/or temperature variability in WOFOST is larger than~~
671 ~~observed. Also, a significant discrepancy emerges in irrigated and rainfed soybean yields,~~
672 ~~where simulated yields surpass the reported values, particularly in rainfed conditions.~~

673 The temporal analysis (Fig. 4) of simulated and reported yields reveals distinct trends and year-
674 to-year fluctuations for each crop. For maize, both irrigated and rainfed conditions show
675 considerable variability in yields over the years. Rainfed maize, in particular, exhibits a
676 discernible pattern with certain years marked by notable peaks in yields, highlighting its
677 sensitivity to varying environmental conditions. These variations are also observed in reported
678 maize yields. This indicates that maize yields, especially under rainfed conditions, are highly
679 influenced by annual climatic variability.

680 For wheat, the simulated yields under both irrigated and rainfed conditions show similar year-
681 to-year patterns, which are not as evident in the reported yields. This suggests that the
682 discrepancies might be due to the model's sensitivity to water and temperature variability,
683 which may not fully capture the complexities of actual wheat production. Specifically, factors
684 such as the use of different wheat varieties, the differentiation between winter and spring wheat,
685 and their respective growth parameters could influence the observed yields. These varietal and
686 seasonal distinctions introduce variability that the model might not fully incorporate, leading
687 to differences between simulated and reported yields.

688 Soybean yields present a different scenario. Both irrigated and rainfed simulated yields
689 consistently surpass the reported values, with the discrepancy being more pronounced in
690 rainfed conditions. This overestimation could be due to the model's assumptions or parameters
691 that do not fully capture the limitations faced by soybean crops in real-world rainfed

environments, such as variations in soil fertility, pest pressures, crop varieties and other management practices not accounted for in the model.

In the spatial analysis (Fig. 5), simulated irrigated maize yields from stand-alone (WOFOST), one-way, and two-way coupling align almost identical with reported irrigated maize yields. Conversely, in rainfed maize analysis, stand-alone and two-way simulations outperform reported yields in states such as Colorado, Kansas, North Dakota, and Wyoming, while one-way coupling exhibits an overestimation of yields compared to stand-alone (WOFOST) and two-way coupling.

For soybeans, the spatial analysis reveals identical yields among stand-alone (WOFOST), one-way, and two-way simulations for both irrigated and rainfed crops. For irrigated crops, simulated yields were overestimated in states like Arkansas and Delaware and underestimated in Kansas and Nebraska compared to reported values. For irrigated and rainfed wheat, simulated yields of the two-way coupling outperform stand-alone WOFOST and one-way coupling, particularly in states like Idaho, Montana, Oregon, and Wyoming. The one-way coupling, lacking feedback from the crop growth model to the hydrological model, leads to an overestimation of rainfed yields across all states compared to stand-alone WOFOST and two-way coupling. This underscores the importance of incorporating two-way interactions and feedback mechanisms for more accurate yield simulation results.

3.2 Evaluation statistics

Table 1 presents model performance metrics (correlation, normalized RMSE and normalized bias), evaluating simulations for the three model setups (i.e. standalone WOFOST, one-way, two-way coupling) for irrigated and rainfed maize, soybean, and wheat.

For irrigated crops, simulation approaches exhibit positive correlations. Specifically, for maize, the correlation coefficients are high (0.63), moderate for soybean and rather low for wheat. The normalized root mean square errors (RMSE) remain consistently low, with values ranging from 0.13 to 0.18 across three crops, indicating a reasonable fit of the simulated values to the observed data. Moreover, normalized biases are also low, ranging from 0.01 to 0.20. The two-way coupling demonstrates overall slightly lower biases compared to stand-alone and one-way simulations, particularly for wheat.

Table 1: Model performance metrics (i.e. correlation, normalized RMSE and normalized bias) for simulated irrigated and rainfed maize, soybean, and wheat.

S.No	Metrics	Maize			Soybean			Wheat		
Irrigated crops		Stand alone	One-way	Two-way	Stand alone	One-way	Two-way	Stand alone	One-way	Two-way
1	Correlation	0.63	0.63	0.63	0.46	0.46	0.45	0.22	0.22	0.24
2	Normalized RMSE	0.13	0.13	0.13	0.06	0.06	0.06	0.18	0.18	0.18
3	Normalized Bias	0.20	0.20	0.20	0.01	0.01	0.01	0.12	0.12	0.06
Rainfed crops		Stand alone	One-way	Two-way	Stand alone	One-way	Two-way	Stand alone	One-way	Two-way
1	Correlation	0.77	0.65	0.77	0.57	0.22	0.33	0.44	0.51	0.55
2	Normalized RMSE	0.22	0.50	0.50	0.42	0.57	0.57	0.37	0.66	0.66
3	Normalized Bias	0.31	1.65	0.84	0.42	0.78	0.63	0.28	0.91	0.32

724

S.NO	Metrics	Maize			Soybean			Wheat		
Irrigated crops		Stand alone	One-way	Two-way	Stand alone	One-way	Two-way	Stand alone	One-way	Two-way
1	Correlation	0.63	0.63	0.63	0.46	0.46	0.45	0.22	0.22	0.24
2	Normalized RMSE	0.13	0.13	0.13	0.06	0.06	0.06	0.18	0.18	0.18
3	Normalized Bias	0.20	0.20	0.20	0.01	0.01	0.01	0.12	0.12	0.06
Rainfed crops		Stand alone	One-way	Two-way	Stand alone	One-way	Two-way	Stand alone	One-way	Two-way
1	Correlation	0.77	0.65	0.77	0.57	0.22	0.33	0.44	0.51	0.55
2	Normalized RMSE	0.22	0.50	0.50	0.42	0.57	0.57	0.37	0.66	0.66
3	Normalized Bias	0.31	1.65	0.84	0.42	0.78	0.63	0.28	0.91	0.32

725

726 For rainfed crops, the correlation coefficients vary, with two-way coupling displaying the
727 highest correlations. Higher correlation coefficients are obtained for maize (0.65-0.77)
728 compared to soybean (0.22-0.57) and wheat (0.44-0.55). Normalized RMSE values are
729 generally higher in rainfed conditions compared to irrigated, ranging from 0.22 to 0.66.
730 Normalized biases show variations across simulation approaches and crops, ranging from 0.28
731 to 1.65. Specifically, one-way coupling exhibits higher biases in rainfed maize, soybean and
732 wheat compared to stand-alone and two-way simulations.

733 Overall, the validation results affirm the overall effectiveness of the simulation approaches in
734 accurately representing observed irrigated and rainfed crop yields, with stand-alone and two-
735 way coupling slightly outperforming one-way simulations.

736 **3.3 Relevant feedbacks revealed by two-way coupling between hydrology and crop**
737 **growth**

738 We further investigated the impact of the developed model coupling by looking at its impact
739 on simulated crop yield in terms of the CONUS-wide 5-arcminute spatial variation and multi-

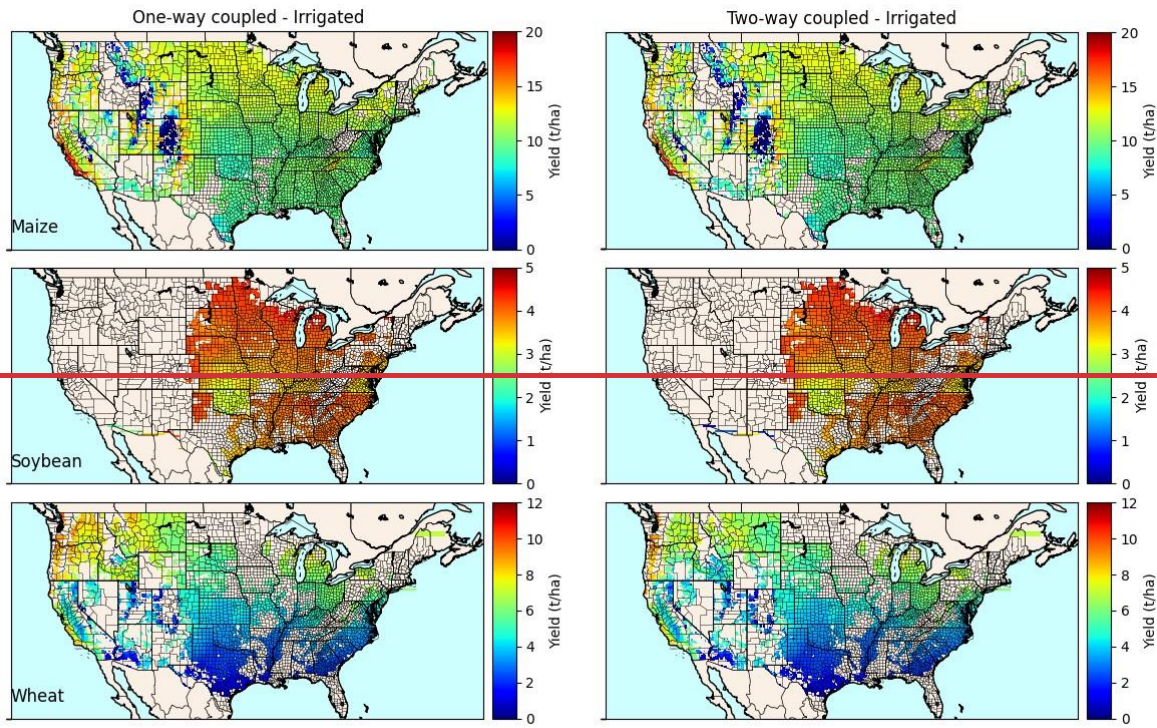
740 year variability. To evaluate the impact of coupling dynamics, we assessed key indicators,
741 including mean crop yields, the coefficient of variation (CV) of crop yields expressing
742 interannual variability, and the relative difference in mean and CV between two-way and one-
743 way couplings.

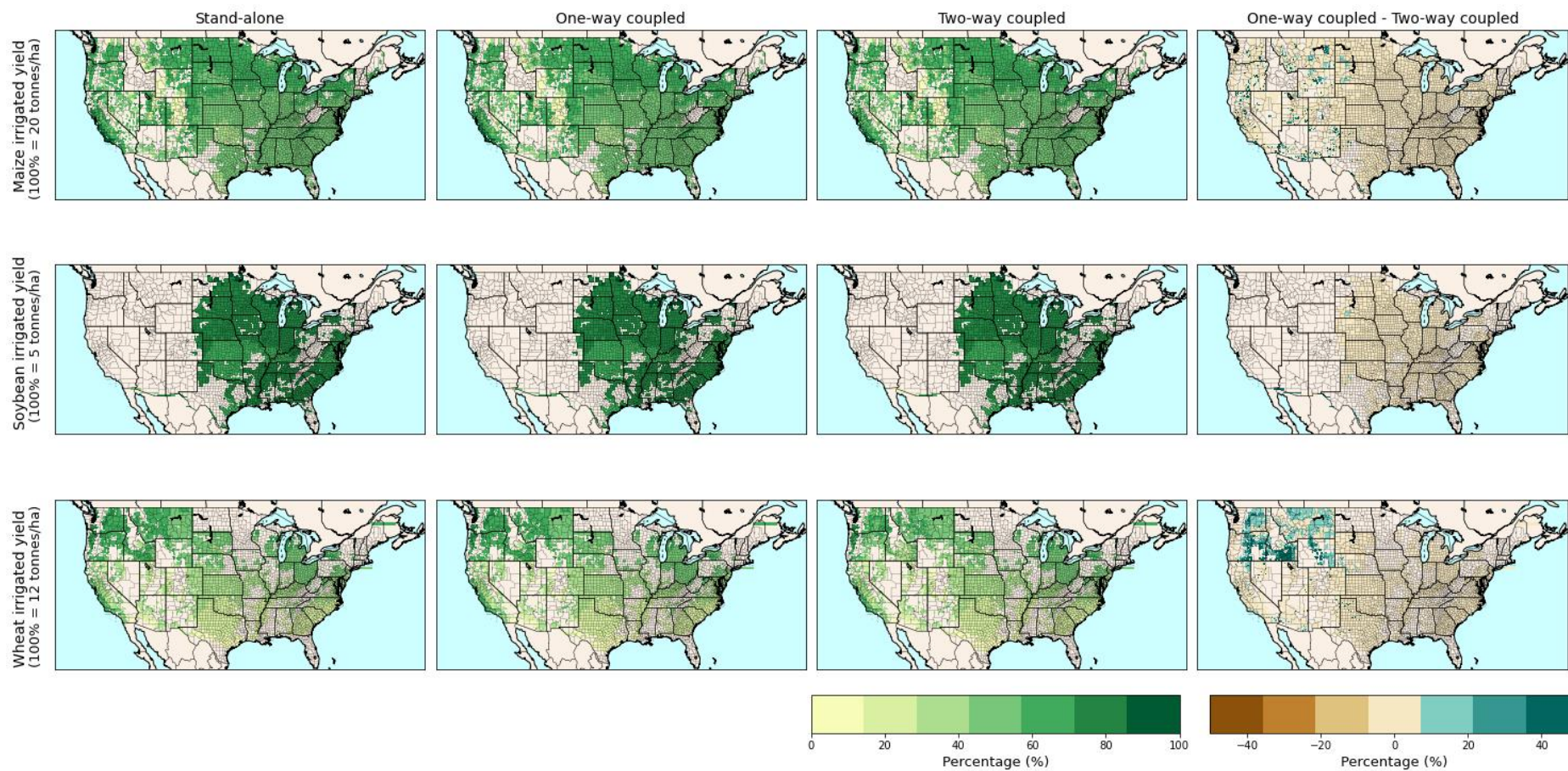
744 Spatial patterns of the 1979-2019 mean simulated crop yields of maize, soybean and wheat are
745 shown under irrigated (Fig. 64) and rainfed (Fig. 75) conditions across the CONUS region. The
746 stand-alone simulations show the yield distribution without coupling between the hydrological
747 and crop models, relying on the internal soil moisture calculation using a simple one-layer
748 tipping bucket approach. In contrast, one-way and two-way coupled simulations involve
749 dynamic interaction between the hydrological model (PCR-GLOBWB 2) and crop growth
750 model (WOFOST), where soil moisture from PCR-GLOBWB 2 is passed to the WOFOST,
751 with two-way coupling also incorporating feedback from WOFOST to the PCR-GLOBWB 2.
752 ~~For irrigated crops (Fig. 4), the regions show similar yields for one-way and two-way coupled~~
753 ~~simulations, which is expected since soil moisture is kept at optimal conditions so that~~
754 ~~feedbacks from WOFOST to PCR-GLOBWB 2 are inconsequential. For irrigated crops (Fig.~~
755 ~~6), the regions show similar yields for stand-alone, one-way and two-way coupled simulations.~~
756 This is expected since soil moisture is kept at optimal levels in irrigated conditions, ensuring
757 that water availability does not become a limiting factor. Consequently, in one-way coupling,
758 the feedback from WOFOST to PCR-GLOBWB 2 is inconsequential, as the continuous supply
759 of water minimizes the need for dynamic interaction between the models.

760 For rainfed conditions (Fig. 57), where water availability relies on green water, the yields are
761 comparatively lower than in irrigated conditions. ~~Also, differences between one-way and two-~~
762 ~~way coupled simulations emerge in the western part of the CONUS. Differences between the~~
763 ~~various coupling approaches become apparent, particularly in the western part of the CONUS.~~
764 Notable differences in yields between stand-alone and two-way simulations are observed in
765 maize and wheat crops, both under irrigated and rainfed conditions. However, these differences
766 are more pronounced in rainfed crops, where water availability is a crucial factor influencing
767 crop yields. In the case of rainfed soybean yields, there is a clear distinction between stand-
768 alone and coupled models, especially in the northern and southern regions of the eastern
769 CONUS. The stand-alone model's tendency to overpredict yields in rainfed conditions
770 underscores the limitation of using a simple one-layer leaky bucket approach in regions where
771 water availability is crucial for crop growth.

772 Notably, one-way coupling tends to simulate higher yields for maize and wheat compared to
773 two-way coupling. This discrepancy arises from the transmission of soil moisture from the
774 hydrological model to the crop growth model in one-way coupling, without receiving feedback
775 from crop development to the hydrological model. As stated before (3.1), this may overestimate
776 soil moisture availability under drier conditions subsequently leading to a likely overestimation
777 of simulated crop yield by the one-way coupling. Clearly, this feedback is more important in
778 the western part of CONUS, which is likely related to larger interannual climate variability
779 (with more dry conditions) compared to the eastern part (see the section hereafter). The larger
780 differences in mean yields for rainfed crops, particularly in the western CONUS, that occur
781 between one-way and two-way coupled simulations are further illustrated by looking at the
782 relative differences between the two coupling methods (see Supplementary Information IV;
783 Fig. S5).

784 Additionally, the two-way coupling reveals that during dry spells, the interaction between
785 declining soil moisture and crop growth leads to an earlier onset of crop stress. In contrast, one-
786 way coupling which does not account for feedback from crop stress to soil moisture, tends to
787 overestimate the severity and timing of water stress on crops. In the two-way coupled
788 simulations, the slower crop development due to water stress in dry years feeds back into the
789 hydrological cycle by reducing evapotranspiration rates. This reduction in evapotranspiration
790 helps conserve soil moisture, thereby influencing the hydrological model's predictions of soil
791 moisture availability. Such feedbacks are absent in one-way coupling, where the fixed
792 phenology leads to an overestimation of water uptake by crops, further exaggerating yield
793 estimates. In some regions of the western CONUS, one-way coupling underestimates yields
794 for rainfed crops of maize and wheat compared to two-way coupling, as the crop growth model
795 WOFOST does not influence hydrological processes in the one-way coupling.

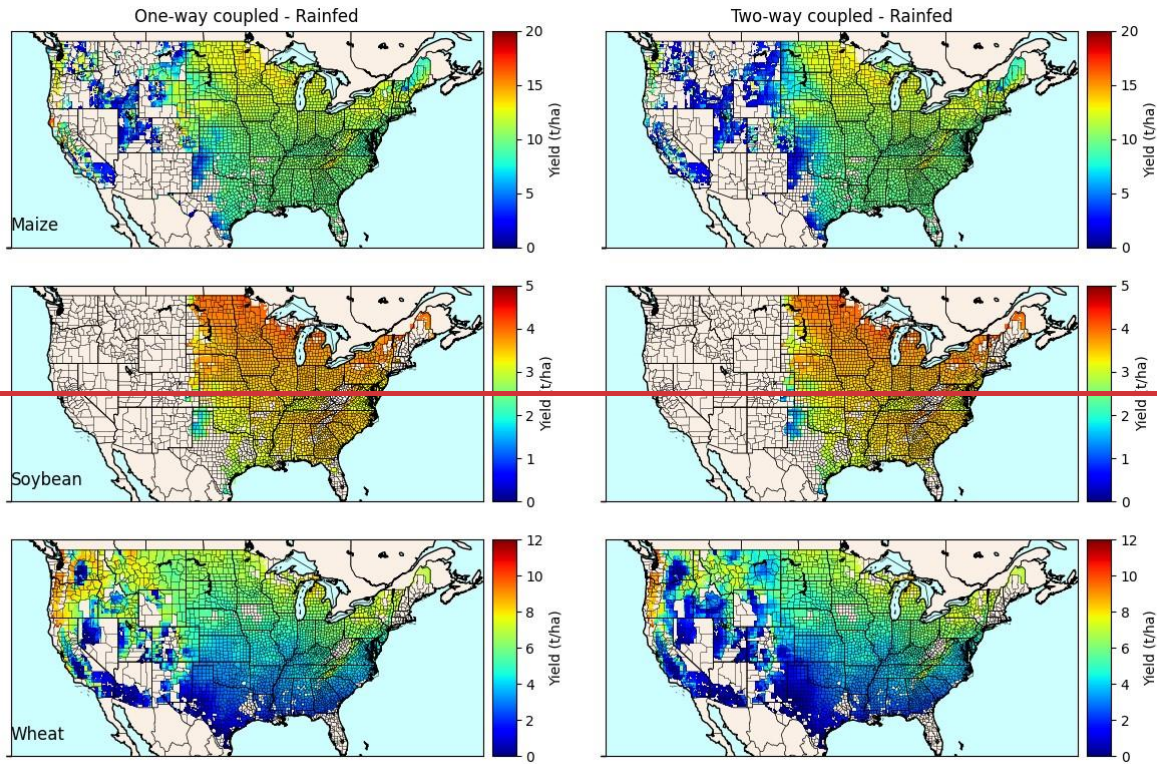




798

799

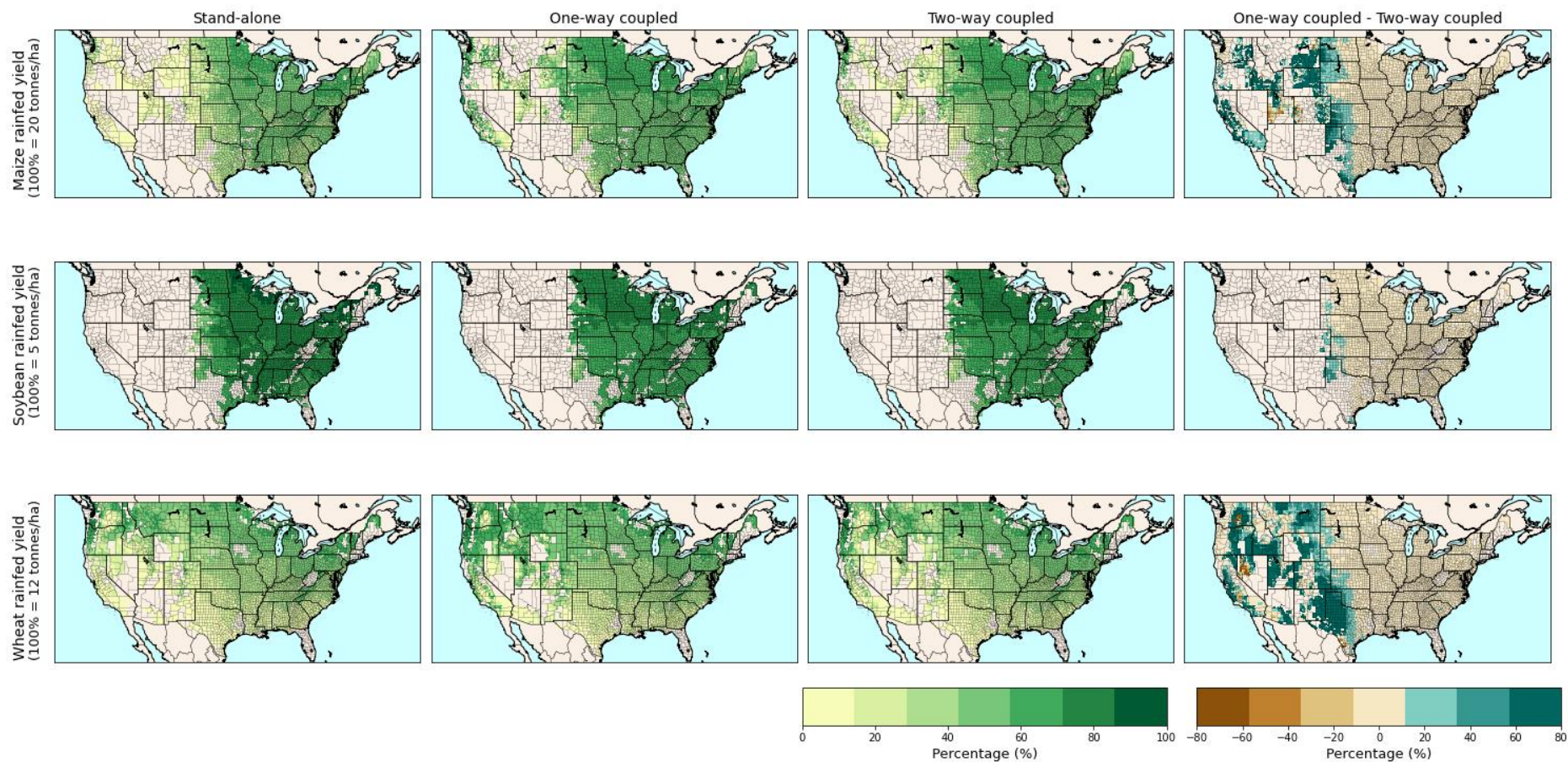
800 **Figure 64:** Mean irrigated crop yields for maize, soybean, and wheat within CONUS as obtained from stand-alone, one-way and two-way coupled simulations and
 801 differences between one-way and two-way coupled simulations for 1979-2019. Legend in % of values shown on the y-axes



802

803

804



805

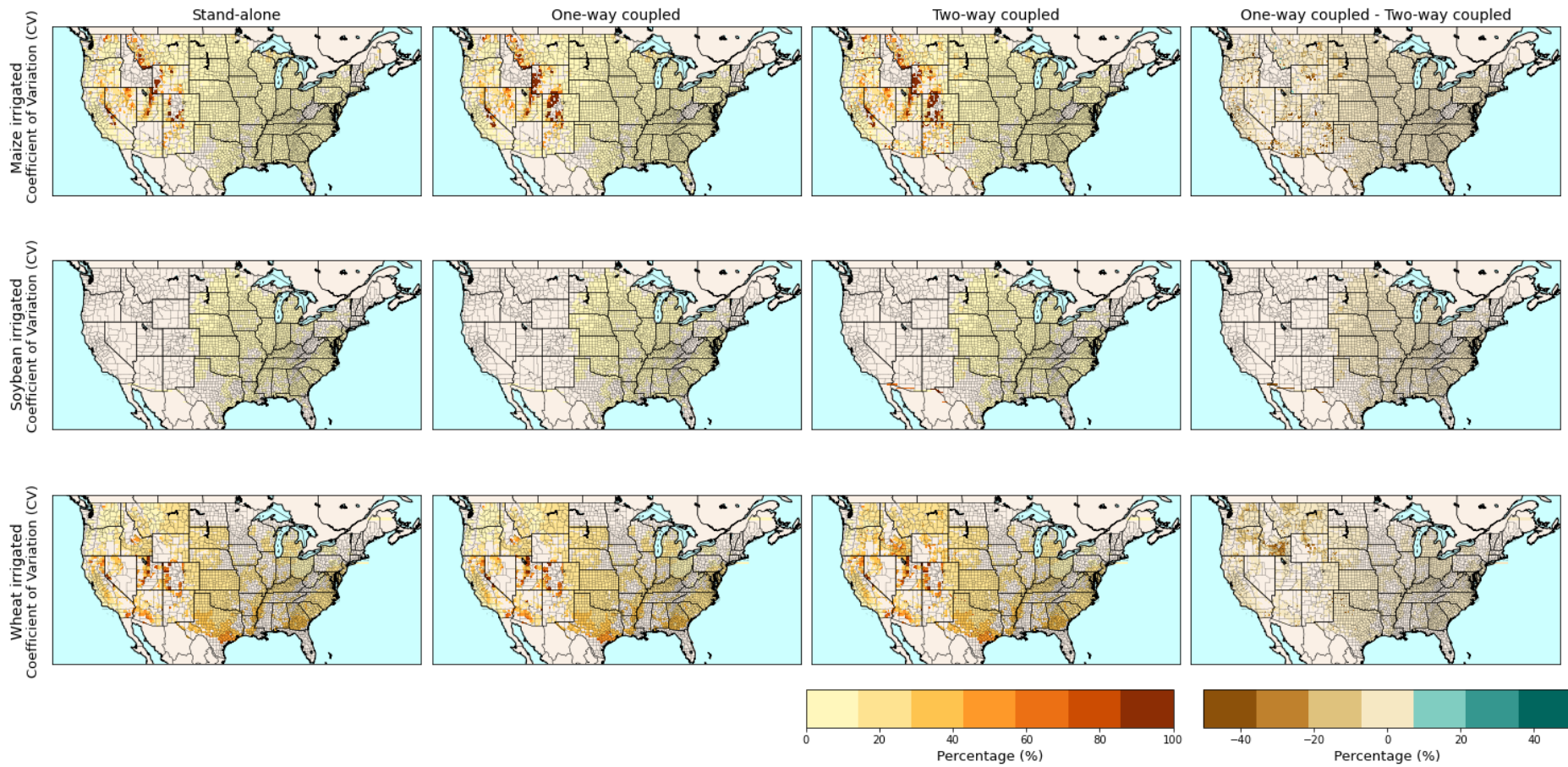
806 **Figure-5 7:** Mean rainfed crop yields for maize, soybean, and wheat within CONUS as obtained from stand-alone, one-way and two-way coupled simulations and
 807 differences between one-way and two-way coupled simulation for 1979-2019. Legend in % of values shown on the y-axes

808

809

810

811

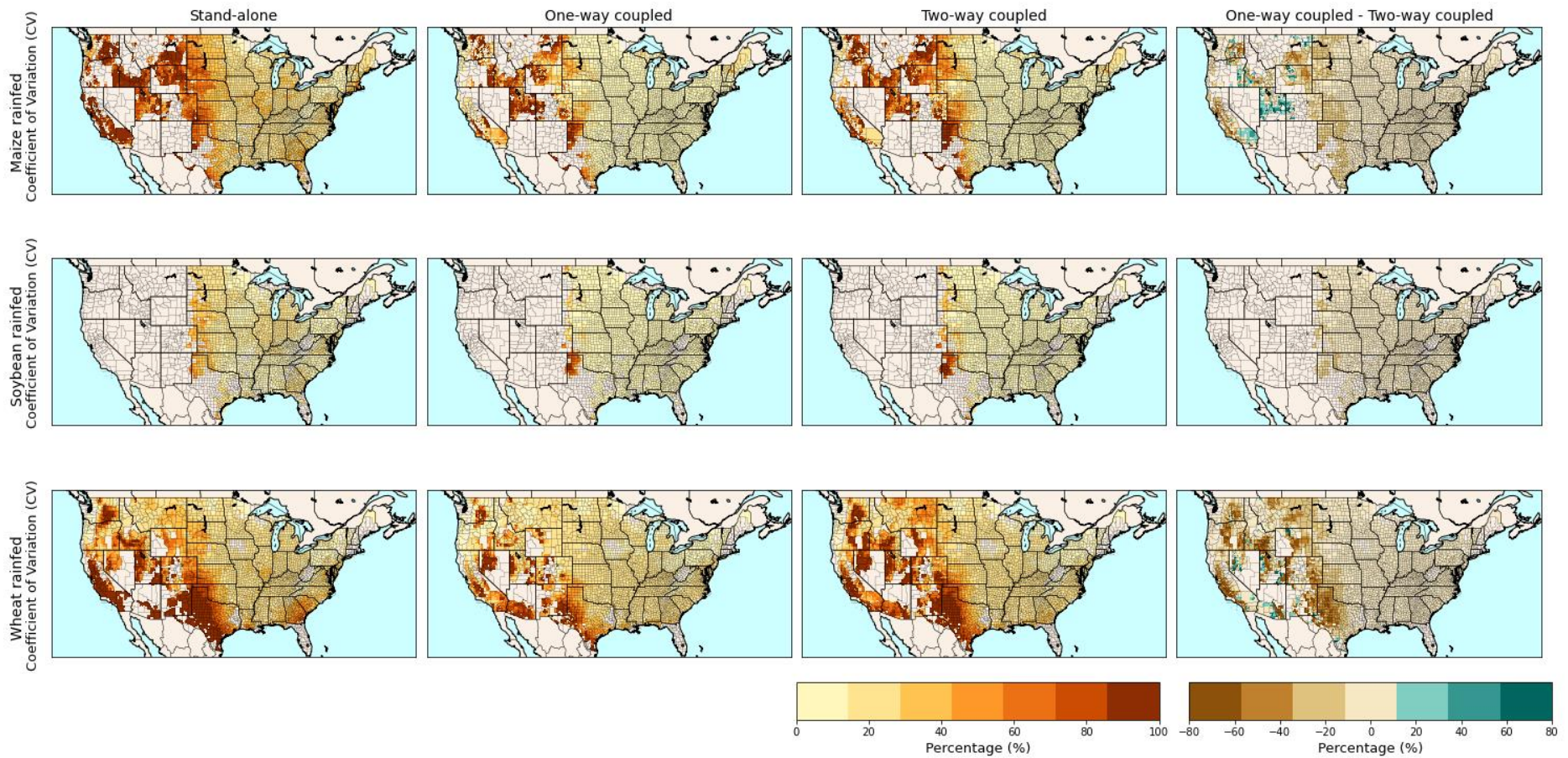


812

813

814 **Figure 8: Coefficient of Variation (CV) over 1979-2019 of irrigated crop yields for maize, soybean, and wheat within CONUS as obtained under stand-alone, one-**
815 **way and two-way coupling and difference between one-way and two-way coupling.**

816

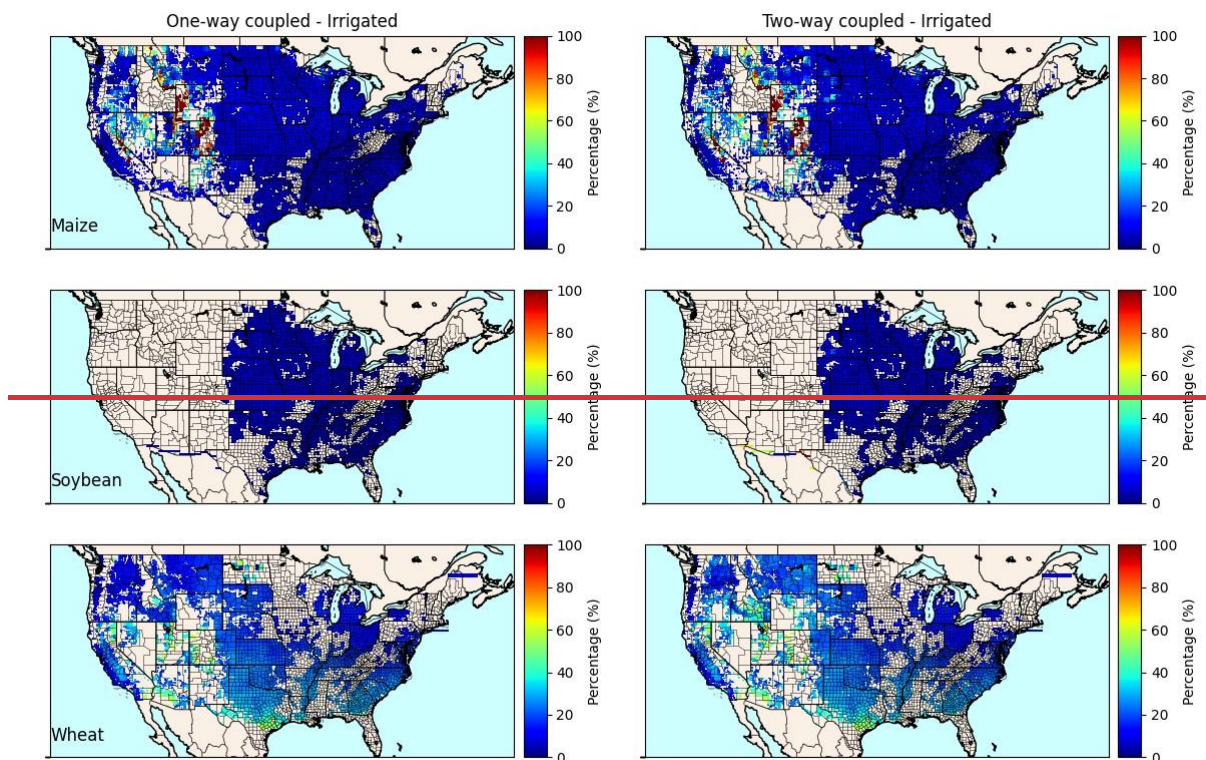


817

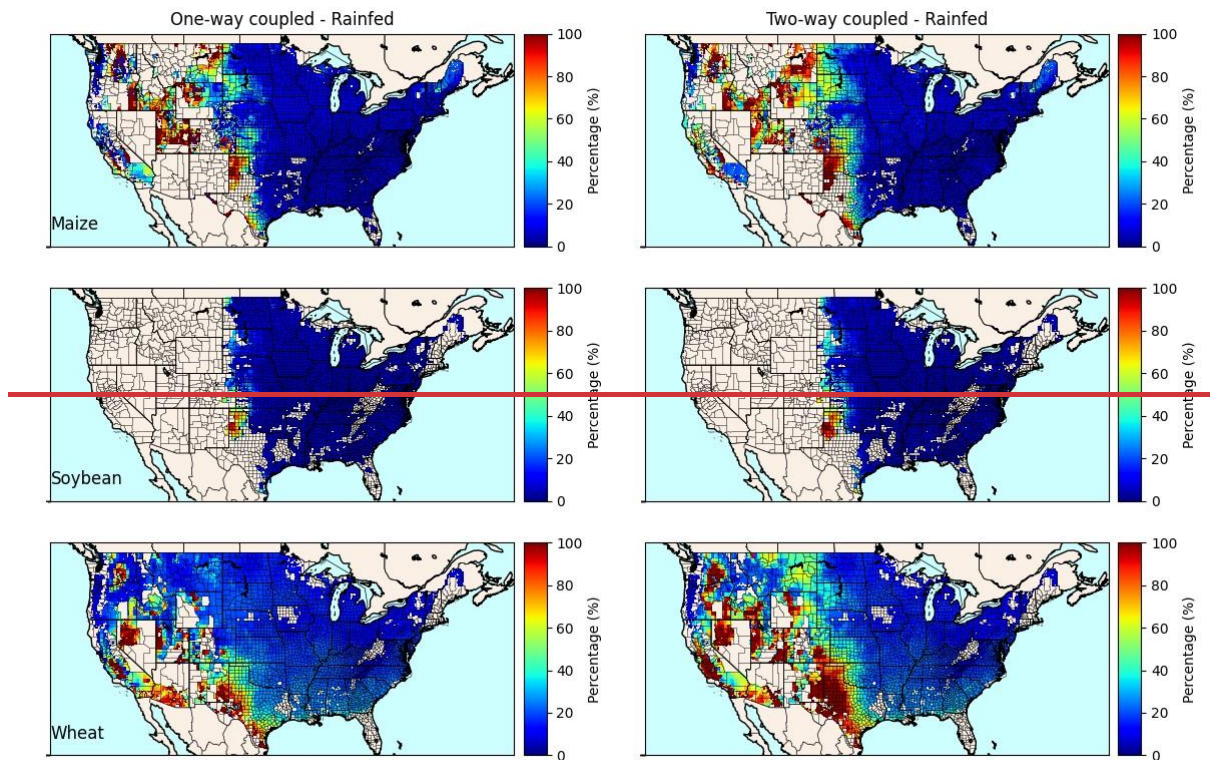
818 **Figure 9: Coefficient of Variation (CV) over 1979-2019 of rainfed crop yields for maize, soybean, and wheat within CONUS as obtained under stand-alone, one-way**
 819 **and two-way coupling and difference between one-way and two-way coupling.**

820 Spatial patterns of the coefficient of variation (CV) (in % of the mean) across CONUS for
821 maize, soybean and wheat are shown under irrigated (Fig. 68) and rainfed conditions (Fig. 79)
822 comparing the simulations of the stand-alone, one-way and two-way coupling. High CV values
823 entail a larger inter-annual variability in crop yield.

824 In the eastern part of CONUS, the CV values both in irrigated and rainfed conditions are
825 notably lower, suggesting a more stable and consistent pattern of crop growth in these regions.
826 Conversely, in the mid-western and western CONUS, inter-annual variability is higher, owing
827 to larger inter-annual climate variability in these parts. For irrigated crops, a larger CV is mostly
828 apparent for maize and wheat. For a small number of instances, this could be caused by
829 insufficient irrigation water availability during very dry and hot years, but most likely this is a
830 temperature signal. Also, we note that in these parts of CONUS, some pixels have very low to
831 minimal cropping areas, resulting in more pronounced fluctuations in yields. As can also be
832 seen from Supplementary Information IV Fig. S6, the differences between one-way and two-
833 way coupled runs are generally small, except for some northwestern states.



834
835 **Figure 6: Coefficient of Variation (CV) over 1979-2019 of irrigated crop yields for maize, soybean, and**
836 **wheat within CONUS as obtained under one-way and two-way coupling**



837

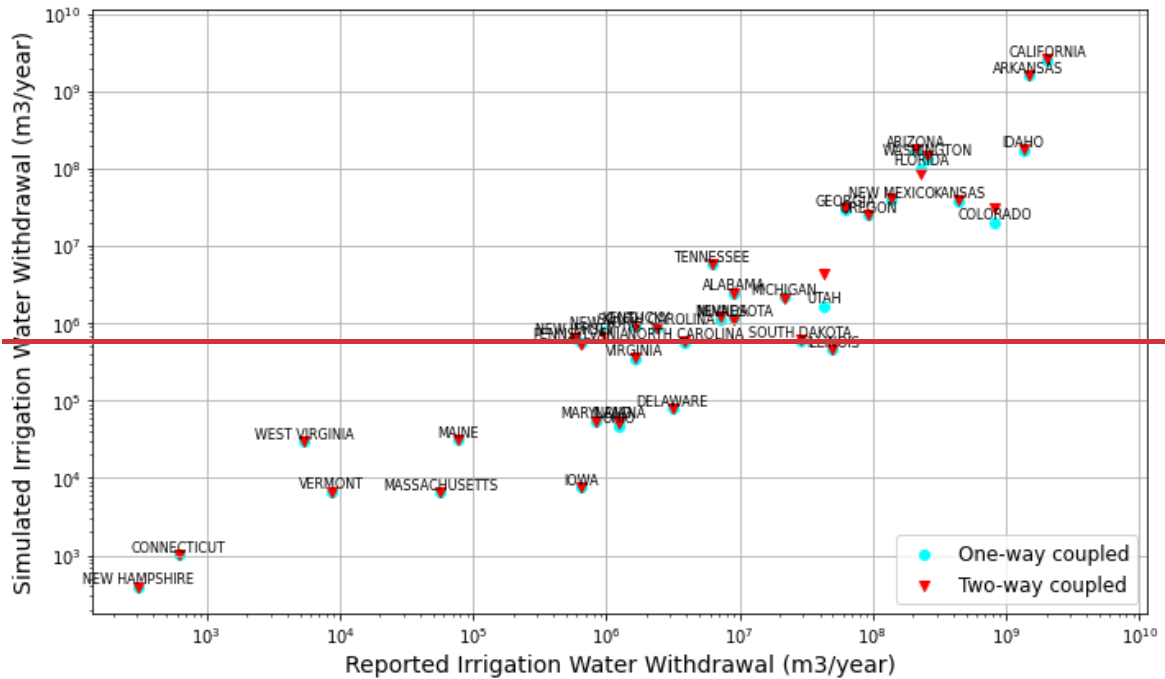
838 **Figure 7: Coefficient of Variation (CV) over 1979–2019 of rainfed crop yields for maize, soybean, and wheat**
 839 **within CONUS as obtained under one-way and two-way coupling**

840 Rainfed crops show larger values of CV, especially in the western part of CONUS, reflecting
 841 the larger sensitivity of rainfed agriculture to inter-annual climate variability (Fig. 97). It is also
 842 clear that the simulated inter-annual variability of simulated crop yield is larger for two-way
 843 than for one-way coupling, reflecting the importance of including crop phenology, in particular
 844 variation in rooting depth, when simulating available soil moisture. We also refer to
 845 Supplementary Information IV Fig. S6 for relative differences between the two model coupling
 846 approaches. This larger inter-annual variability also partly explains the lower mean yields for
 847 rainfed crops and two-way coupling as was shown in Fig 57.

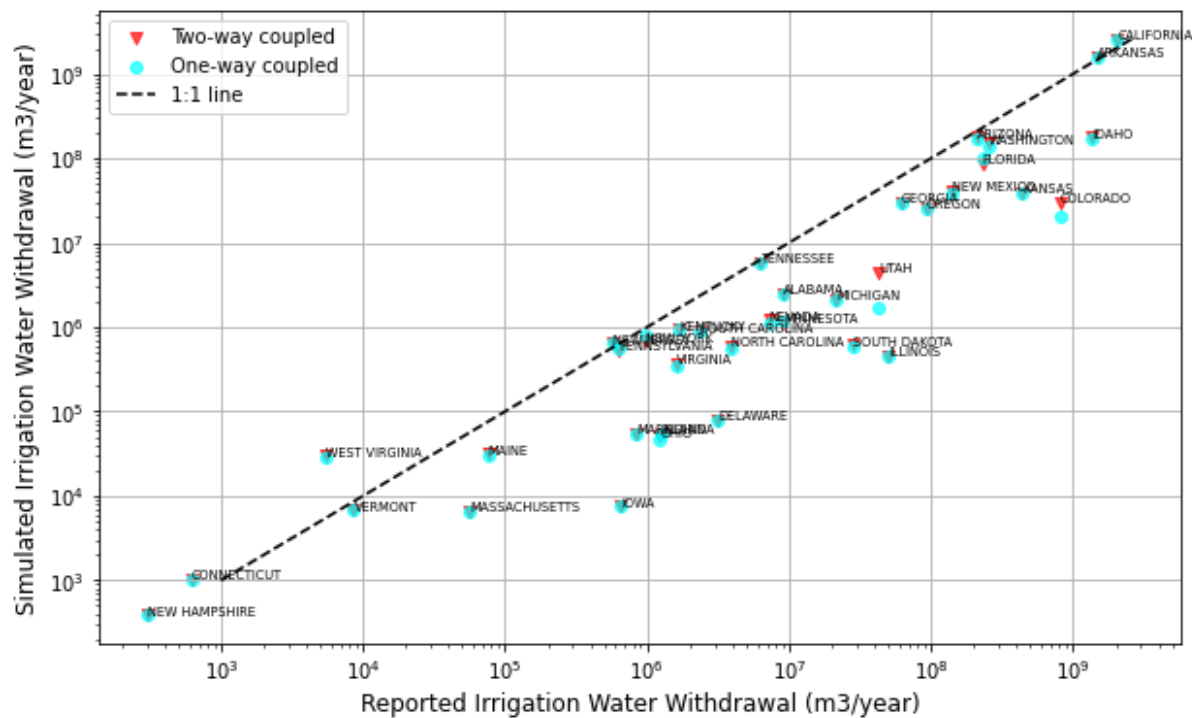
848 3.4 Irrigation water use

849 The scatter plot (Fig. 810) shows the relationship between reported USGS (after correction for
 850 area and irrigation efficiency – see 2.45.2) and simulated irrigation water withdrawals under
 851 one-way and two-way coupling. The plot shows that the simulated irrigation water withdrawals
 852 are correct in order of magnitude when compared to reported data across different states. The
 853 temporal variations (Fig. 911) illustrate that year-to-year changes in total irrigation water
 854 withdrawal over time are small for both one-way and two-way coupling and the reported totals.

855 Figures 108 and 911 show that irrigation water withdrawal is underestimated in total and for
 856 most states. The underestimation of irrigation water use by PCR-GLOBWB 2 was previously
 857 noted by Ruess et al., (2023). This underestimation was partly accounted for when using more
 858 detailed crop cover data, irrigation efficacies and meteorological forcing than currently used in
 859 the global version of PCR-GLOBWB 2.

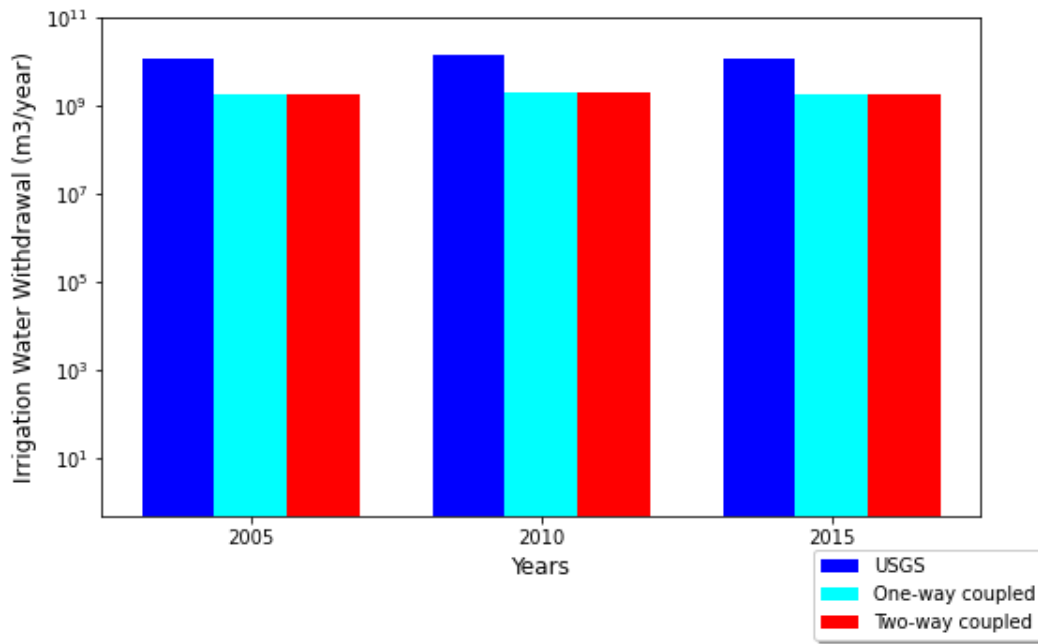


860



861

862 **Figure 810:** Spatial variation of one-way and two-way irrigation water withdrawal compared with USGS-
 863 **reported** water withdrawal data **per state for all crops** across the CONUS region with a logarithmic scale



864

865 **Figure 911:** Temporal variation of one-way and two-way irrigation water withdrawal compared with USGS
 866 water withdrawal data of 5-year intervals across the CONUS region with a logarithmic scale

867 **4 Discussion and Conclusion**

868 In this study, we developed a coupled hydrological-crop model framework to investigate the
 869 intricate feedbacks between water availability and crop growth within the CONUS region
 870 focusing on maize, soybean and wheat. This discussion delves into the implications of the
 871 findings, emphasizing their significance and addressing both methodological considerations
 872 and inherent uncertainties.

873 The spatiotemporal analysis of hydrological impacts on crop growth reveals distinctive patterns
 874 for both irrigated and rainfed conditions. Notably, the improved performance of the two-way
 875 coupling in capturing more realistic yield outcomes for rainfed conditions highlights the
 876 importance of incorporating the full feedback loop between hydrology and crop growth. The
 877 discrepancy in one-way coupling results, leading to overestimation in simulated compared to
 878 reported yields, underscores the importance of feeding back the actual crop phenology to the
 879 hydrological model in coupled hydrological-crop growth modelling.

880 Our studies adds to previous work by Droppers et al., (2021), which investigated worldwide
 881 water constraints and sustainable irrigation by coupling the Variable Infiltration Capacity
 882 (VIC) hydrological model with WOFOST and Zhang et al. (2021) who focused on refining the
 883 coupled VIC hydrological model with a crop growth model EPIC by incorporating the
 884 evapotranspiration module at a regional scale. In comparison, our research extends the analysis
 885 to a finer spatial scale and places a stronger emphasis on the comprehensive integration of

886 feedback loops between hydrology and crop growth. Particularly, we demonstrate the
887 importance of two-way coupling in capturing realistic yield outcomes, which is particularly
888 evident for rainfed crops. This is mainly because the two-way coupled system addresses the
889 influence of crop status on evapotranspiration and rooting depth, thereby impacting soil
890 moisture content, which in turn feed backs on crop growth. The two-way coupling approach
891 provides a more realistic depiction of water availability for crops, which results in larger inter-
892 annual variability and lower mean crop yields when inter-annual climate variability is
893 significant. Including this two-way interaction is particularly important under drier conditions
894 or if the coupled framework is used to assess reduced surface water availability under climate
895 change or the impact of environmental constraints on groundwater and surface water use. The
896 significance of implementing a two-way coupling between hydrology and crop growth is also
897 evident when calculating high-resolution long-term mean crop yields and inter-annual
898 variability of yield, as measured by the coefficient of variation (CV) of simulated yield. In
899 irrigated conditions, both one-way and two-way coupling yield similar results, demonstrating
900 the stability in water availability.

901 Validation results affirm the reliability of the coupled PCR-GLOBWB 2 – WOFOST model
902 framework, demonstrating close agreement with observed data through overall strong positive
903 correlations, low normalized RMSE, and minimal bias. Here, the difference in performance
904 between one-way and two-way coupling is small. In rainfed conditions, where variability is
905 inherent, the better performance of two-way coupling emphasizes the added value of dynamic
906 feedback mechanisms for more accurate simulation results. Even though the stand-alone
907 WOFOST performed similarly to the two-way coupled model framework, the latter is still
908 beneficial for comprehensively understanding the joint impacts on both crop growth and
909 irrigation water use, particularly in situations of limited water availability.

910 While the results of this study offer valuable insights into the coupled hydrological-crop
911 model framework, it is essential to recognize and address the uncertainties associated with the
912 structure and parametrization, as well as inherent limitations in the research. A significant
913 limitation is that the study does not account for potential advancements in agricultural
914 technology and evolving farming practices, which could impact crop yields (section 3.1; Fig.
915 2). The ignorance of technological innovations may contribute to discrepancies between
916 simulated and actual yields.

917 Furthermore, uncertainties linked to input datasets (Porwollik et al., 2017; Roux et al., 2014)
918 such as crop calendars, cultivars and land-use changes introduce potential limitations and
919 implications for the study results. Accurate representations of crop growth dynamics hinge on
920 accurate crop calendar definitions (Wang et al., 2022), encompassing planting, maturation, and
921 harvesting periods. Variations in these timelines due to climate change or evolving agricultural
922 practices potentially introduce uncertainties in yield predictions. Additionally, the assumption
923 of static cultivars neglects potential shifts in agricultural practices or the introduction of new
924 varieties, influencing crop growth responses to environmental stressors over time. Land-use
925 changes further contribute to uncertainties (Prestele et al., 2016; Eckhardt et al., 2003;
926 Dendoncker et al., 2008) as dynamic shifts in agricultural practices alter water demand,
927 evapotranspiration patterns, and overall hydrological dynamics. Ignoring these potential shifts
928 limits the model's ability to capture the complex interactions between water and crop systems,
929 and this should be considered in future development steps.

930 Hence, future work should also consider representing the dynamic nature of crop areas,
931 including both irrigated and rainfed crop harvest areas, as well as the total crop area. The
932 assumption of constant areas, as made in prior studies (Müller et al., 2017; Ai and Hanasaki,
933 2023; Jägermeyr et al., 2021) was based on data availability constraints, but acknowledging
934 the potential variability in these factors over time. Addressing this aspect is crucial for
935 enhancing the accuracy of yield calculations and, consequently, advancing the overall
936 understanding of hydrologically-crop growth interactions. The integration of such variability
937 into modelling frameworks is not only essential for improving the accuracy of assessments but
938 also for contributing to an enhanced understanding of the broader water-food nexus.

939 Additionally, within the nexus context, the developed coupled framework can be integrated
940 into various models across different programming languages, providing a flexible and
941 adaptable tool to address a wide range of research needs.

942 In conclusion, the development and application of the two-way coupled hydrological-crop
943 growth model framework presented in this study represents a significant advancement in our
944 ability to understand the cascading mechanisms and feedbacks between water and crop
945 systems. This versatile framework not only enhances our understanding of the interplay
946 between hydrology and crop growth but, through the sectoral water use modules of PCR-
947 GLOBWB 2, has the necessary components to evaluate large-scale water use management
948 strategies, and simulate the large-scale impacts of informed decision-making under change,
949 particularly when dealing with hydroclimatic extremes.

950

951 **Author contribution**

952 SC designed the study, performed the analyses, validation and visualization of the results under
953 the supervision of LPHvB, MTHvV and MFPB. SC developed the coupled framework in close
954 collaboration with LPHvB. JA contributed to the conceptualization of software. SC wrote the
955 original draft manuscript and all co-authors reviewed and edited the manuscript.

956 **Code and data availability**

957 The developed coupled PCR-GLOBWB 2-WOFOST model framework is available at
958 <https://zenodo.org/doi/10.5281/zenodo.10681452>. The datasets used in the coupled model
959 framework are available at
960 [https://opendap.4tu.nl/thredds/catalog/data2/pcrglobwb/version_2019_11_beta/pcrglobwb2_i](https://opendap.4tu.nl/thredds/catalog/data2/pcrglobwb/version_2019_11_beta/pcrglobwb2_input/catalog.html)
961 [nput/catalog.html](https://opendap.4tu.nl/thredds/catalog/data2/pcrglobwb/version_2019_11_beta/pcrglobwb2_input/catalog.html).

962 **Competing interests**

963 The contact author has declared that none of the authors has any competing interests.

964 **Acknowledgement**

965 The authors acknowledge dr. Bram Droppers (Utrecht University) and dr. Iwan Supit
966 (Wageningen University) for their valuable advices on the WOFOST crop model.

967 **Financial support**

968 This research has been funded by the European Union Horizon Programme GoNexus project
969 (Grant Agreement Number 101003722). MTHvV was financially supported by the Netherlands
970 Scientific Organisation (NWO) by a VIDI grant (VI.Vidi.193.019) and the European Research
971 Council (ERC) under the European Union's Horizon Europe research and innovation program
972 (grant agreement 101039426 B-WEX).

973

974 **5 References**

- 975 Ai, Z., & Hanasaki, N. (2023). Simulation of crop yield using the global hydrological model H08 (crp.v1).
976 *Geoscientific Model Development*, 16(11), 3275–3290. <https://doi.org/10.5194/gmd-16-3275-2023>
- 977 Antle, J. M., Capalbo, S. M., Elliott, E. T., Hunt, H. W., Mooney, S., & Paustian, K. H. (2001). Research needs
978 for understanding and predicting the behavior of managed ecosystems: lessons from the study of
979 agroecosystems. *Ecosystems*, 4, 723–735.
- 980 Arata, L., Fabrizi, E., & Sckokai, P. (2020). A worldwide analysis of trend in crop yields and yield variability:
981 Evidence from FAO data. *Economic Modelling*, 90, 190–208.
982 <https://doi.org/10.1016/J.ECONMOD.2020.05.006>

- 983 CSDMS: <https://babelizer.readthedocs.io/en/latest/>, last access: 06 February 2024.
- 984 Corona-López, E., Román-Gutiérrez, A. D., Otazo-Sánchez, E. M., Guzmán-Ortiz, F. A., & Acevedo-Sandoval,
985 O. A. (2021). Water–food nexus assessment in agriculture: A systematic review. *International Journal of*
986 *Environmental Research and Public Health*, 18(9), 1–14. <https://doi.org/10.3390/ijerph18094983>
- 987 de Wit, A., & Boogaard, H. (2021). A Gentle Introduction to WOFOST. November, 287–295.
988 https://doi.org/10.1007/978-3-319-06956-2_25
- 989 de Wit, A., Boogaard, H., Fumagalli, D., Janssen, S., Knapen, R., van Kraalingen, D., Supit, I., van der Wijngaart,
990 R., & van Diepen, K. (2019). 25 years of the WOFOST cropping systems model. *Agricultural Systems*,
991 168(October 2017), 154–167. <https://doi.org/10.1016/j.agry.2018.06.018>
- 992 Dendoncker, N., Schmit, C., & Rounsevell, M. (2008). Exploring spatial data uncertainties in land-use change
993 scenarios. *International Journal of Geographical Information Science*, 22(9), 1013–1030.
994 <https://doi.org/10.1080/13658810701812836>
- 995 Droppers, B., Supit, I., Van Vliet, M. T. H., & Ludwig, F. (2021). Worldwide water constraints on attainable
996 irrigated production for major crops. *Environmental Research Letters*, 16(5). <https://doi.org/10.1088/1748-9326/abf527>
- 998 Dubois, O. (2011). The state of the world’s land and water resources for food and agriculture: managing systems
999 at risk. Earthscan.
- 1000 Easterling, W. E. (1997). Why regional studies are needed in the development of full-scale integrated assessment
1001 modelling of global change processes. *Global Environmental Change*, 7(4), 337–356.
1002 [https://doi.org/10.1016/S0959-3780\(97\)00016-2](https://doi.org/10.1016/S0959-3780(97)00016-2)
- 1003 Eckhardt, K., Breuer, L., & Frede, H. G. (2003). Parameter uncertainty and the significance of simulated land use
1004 change effects. *Journal of Hydrology*, 273(1–4), 164–176. [https://doi.org/10.1016/S0022-1694\(02\)00395-5](https://doi.org/10.1016/S0022-1694(02)00395-5)
- 1005 Ewert, F., Rötter, R. P., Bindi, M., Webber, H., Trnka, M., Kersebaum, K. C., Olesen, J. E., van Ittersum, M. K.,
1006 Janssen, S., Rivington, M., Semenov, M. A., Wallach, D., Porter, J. R., Stewart, D., Verhagen, J., Gaiser,
1007 T., Palosuo, T., Tao, F., Nendel, C., ... Asseng, S. (2015). Crop modelling for integrated assessment of risk
1008 to food production from climate change. *Environmental Modelling & Software*, 72, 287–303.
1009 <https://doi.org/10.1016/J.ENVSOFT.2014.12.003>
- 1010 Huang, J., Hartemink, A. E., & Kucharik, C. J. (2021). Soil-dependent responses of US crop yields to climate
1011 variability and depth to groundwater. *Agricultural Systems*, 190, 103085.
1012 <https://doi.org/10.1016/J.AGSY.2021.103085>
- 1013 Hutton, E., Piper, M., & Tucker, G. (2020). The Basic Model Interface 2.0: A standard interface for coupling
1014 numerical models in the geosciences. *Journal of Open Source Software*, 5(51), 2317.
1015 <https://doi.org/10.21105/joss.02317>
- 1016 IRENA. (2015). Renewable energy in the water, energy and food nexus. International Renewable Energy Agency,
1017 January, 1–125.
- 1018 Jackson, N. D., Konar, M., Debaere, P., & Sheffield, J. (2021). Crop-specific exposure to extreme temperature
1019 and moisture for the globe for the last half century. *Environmental Research Letters*, 16(6), 064006.
1020 <https://doi.org/10.1088/1748-9326/ABF8E0>
- 1021 Jägermeyr, J., Pastor, A., Biemans, H., & Gerten, D. (2017). Reconciling irrigated food production with
1022 environmental flows for Sustainable Development Goals implementation. *Nature Communications*,
1023 8(May), 1–9. <https://doi.org/10.1038/ncomms15900>
- 1024 Kanda, E. K., Mabhaudhi, T., & Senzanje, A. (2018). Coupling hydrological and crop models for improved
1025 agricultural water management – A review. *Bulgarian Journal of Agricultural Science*, 24(3), 380–390.
- 1026 Lange et al. (2021). Lange, S., Menz, C., Gleixner, S., Cucchi, M., Weedon, G. P., Amici, A., Bellouin, N.,
1027 Schmied, H. M., Hersbach, H., Buontempo, C., & Cagnazzo, C. (2021). WFDE5 over land merged with
1028 ERA5 over the ocean (W5E5 v2.0). 2021.
- 1029 Leclère, D., Havlík, P., Fuss, S., Schmid, E., Mosnier, A., Walsh, B., Valin, H., Herrero, M., Khabarov, N., &
1030 Obersteiner, M. (2014). Climate change induced transformations of agricultural systems: Insights from a

- 1031 global model. *Environmental Research Letters*, 9(12). <https://doi.org/10.1088/1748-9326/9/12/124018>
- 1032 Li, Y., Zhou, Q., Zhou, J., Zhang, G., Chen, C., & Wang, J. (2014). Assimilating remote sensing information into
1033 a coupled hydrology-crop growth model to estimate regional maize yield in arid regions. *Ecological*
1034 *Modelling*, 291, 15–27.
- 1035 McMillan, H. K., Westerberg, I. K., & Krueger, T. (2018). Hydrological data uncertainty and its implications.
1036 *Wiley Interdisciplinary Reviews: Water*, 5(6), 1–14. <https://doi.org/10.1002/WAT2.1319>
- 1037 Momblanch, A., Papadimitriou, L., Jain, S. K., Kulkarni, A., Ojha, C. S. P., Adeloje, A. J., & Holman, I. P.
1038 (2019). Science of the Total Environment Untangling the water-food-energy-environment nexus for global
1039 change adaptation in a complex Himalayan water resource system. *Science of the Total Environment*, 655,
1040 35–47. <https://doi.org/10.1016/j.scitotenv.2018.11.045>
- 1041 Mortada, S., Abou Najm, M., Yassine, A., El Fadel, M., & Alamiddine, I. (2018). Towards sustainable water-
1042 food nexus: An optimization approach. *Journal of Cleaner Production*, 178, 408–418.
1043 <https://doi.org/10.1016/J.JCLEPRO.2018.01.020>
- 1044 Müller, C., Elliott, J., Chryssanthacopoulos, J., Arneth, A., Balkovic, J., Ciais, P., Deryng, D., Folberth, C.,
1045 Glotter, M., Hoek, S., Iizumi, T., Izaurrealde, R. C., Jones, C., Khabarov, N., Lawrence, P., Liu, W., Olin,
1046 S., Pugh, T. A. M., Ray, D. K., ... Yang, H. (2017). Global gridded crop model evaluation: Benchmarking,
1047 skills, deficiencies and implications. *Geoscientific Model Development*, 10(4), 1403–1422.
1048 <https://doi.org/10.5194/gmd-10-1403-2017>
- 1049 Peckham, S. D., Hutton, E. W. H., & Norris, B. (2013). A component-based approach to integrated modeling in
1050 the geosciences: The design of CSDMS. *Computers & Geosciences*, 53, 3–12.
1051 <https://doi.org/10.1016/J.CAGEO.2012.04.002>
- 1052 Portmann, F. T., Siebert, S., & Döll, P. (2010). MIRCA2000—Global monthly irrigated and rainfed crop areas
1053 around the year 2000: A new high-resolution data set for agricultural and hydrological modeling. *Global*
1054 *Biogeochemical Cycles*, 24(1), 1–24. <https://doi.org/10.1029/2008gb003435>
- 1055 Porwollik, V., Müller, C., Elliott, J., Chryssanthacopoulos, J., Iizumi, T., Ray, D. K., Ruane, A. C., Arneth, A.,
1056 Balković, J., Ciais, P., Deryng, D., Folberth, C., Izaurrealde, R. C., Jones, C. D., Khabarov, N., Lawrence, P.
1057 J., Liu, W., Pugh, T. A. M., Reddy, A., ... Wu, X. (2017). Spatial and temporal uncertainty of crop yield
1058 aggregations. *European Journal of Agronomy*, 88, 10–21. <https://doi.org/10.1016/J.EJA.2016.08.006>
- 1059 Prestele, R., Alexander, P., Rounsevell, M. D. A., Arneth, A., Calvin, K., Doelman, J., Eitelberg, D. A., Engström,
1060 K., Fujimori, S., Hasegawa, T., Havlik, P., Humpenöder, F., Jain, A. K., Krisztin, T., Kyle, P., Meiyappan,
1061 P., Popp, A., Sands, R. D., Schaldach, R., ... Verburg, P. H. (2016). Hotspots of uncertainty in land-use and
1062 land-cover change projections: a global-scale model comparison. *Global Change Biology*, 22(12), 3967–
1063 3983. <https://doi.org/10.1111/gcb.13337>
- 1064 Roux, S., Brun, F., & Wallach, D. (2014). Combining input uncertainty and residual error in crop model
1065 predictions: A case study on vineyards. *European Journal of Agronomy*, 52, 191–197.
1066 <https://doi.org/10.1016/J.EJA.2013.09.008>
- 1067 Ruess, P. J., Konar, M., Wanders, N., & Bierkens, M. (2023). Irrigation by Crop in the Continental United States
1068 From 2008 to 2020. *Water Resources Research*, 59(2), 1–19. <https://doi.org/10.1029/2022WR032804>
- 1069 Shafiei, M., Ghahraman, B., Saghafian, B., Davary, K., Pande, S., & Vazifedoust, M. (2014). Uncertainty
1070 assessment of the agro-hydrological SWAP model application at field scale: A case study in a dry region.
1071 *Agricultural Water Management*, 146, 324–334. <https://doi.org/10.1016/J.AGWAT.2014.09.008>
- 1072 Siad, S. M., Iacobellis, V., Zdruli, P., Gioia, A., Stavi, I., & Hoogenboom, G. (2019). A review of coupled
1073 hydrologic and crop growth models. *Agricultural Water Management*, 224, 105746.
1074 <https://doi.org/10.1016/J.AGWAT.2019.105746>
- 1075 Sophocleous, M. (2004). *Global and Regional Water Availability and Demand : Prospects for the Future*. 13(2).
- 1076 Supit, I., Hooijer, A. A., & van Diepen, C. A. (Eds. . (1994). System description of the WOFOST 6.0 crop
1077 simulation model implemented in CGMS Vol. 1: Theory and Algorithms. EUR Publication 15956,
1078 Agricultural Series, Luxembourg, 146 Pp., 1(October 2015), 181.
1079 <https://cir.nii.ac.jp/crid/1573950399770954368>

1080 Sutanudjaja, E. H., Van Beek, R., Wanders, N., Wada, Y., Bosmans, J. H. C., Drost, N., Van Der Ent, R. J., De
1081 Graaf, I. E. M., Hoch, J. M., De Jong, K., Karssenberg, D., López López, P., Peßenteiner, S., Schmitz, O.,
1082 Straatsma, M. W., Vannamete, E., Wisser, D., & Bierkens, M. F. P. (2018). PCR-GLOBWB 2: A 5 arcmin
1083 global hydrological and water resources model. *Geoscientific Model Development*, 11(6), 2429–2453.
1084 <https://doi.org/10.5194/gmd-11-2429-2018>

1085 Tompkins, E. L., & Adger, W. N. (2004). Does Adaptive Management of Natural Resources Enhance Resilience
1086 to Climate Change? *9*(2).

1087 Tsarouchi, G. M., Buytaert, W., & Mijic, A. (2014). Coupling a land-surface model with a crop growth model to
1088 improve ET flux estimations in the Upper Ganges basin, India. 4223–4238. <https://doi.org/10.5194/hess-18-4223-2014>

1090 USGS, 2023. Water use in the United States, from USGS Water-Science School. 1–2.

1091 USDA: <https://quickstats.nass.usda.gov/>, last access: 06 February 2024.

1092 Veettil, A. V., Mishra, A. K., & Green, T. R. (2022). Explaining water security indicators using hydrologic and
1093 agricultural systems models. *Journal of Hydrology*, 607, 127463.
1094 <https://doi.org/10.1016/J.JHYDROL.2022.127463>

1095 Vereecken, H., Schnepf, A., Hopmans, J. W., Javaux, M., Or, D., Roose, T., Vanderborght, J., Young, M. H.,
1096 Amelung, W., & Aitkenhead, M. (2016). Modeling soil processes: Review, key challenges, and new
1097 perspectives. *Vadose Zone Journal*, 15(5), vzj2015-09.

1098 Vörösmarty, C. J., Green, P., Salisbury, J., & Lammers, R. B. (2000). Global water resources: Vulnerability from
1099 climate change and population growth. *Science*, 289(5477), 284–288.
1100 <https://doi.org/10.1126/science.289.5477.284>

1101 Wang, Xiaobo, Folberth, C., Skalsky, R., Wang, S., Chen, B., Liu, Y., Chen, J., & Balkovic, J. (2022). Crop
1102 calendar optimization for climate change adaptation in rice-based multiple cropping systems of India and
1103 Bangladesh. *Agricultural and Forest Meteorology*, 315, 108830.
1104 <https://doi.org/10.1016/J.AGRFORMET.2022.108830>

1105 Wang, Xiuying, Williams, J. R., Gassman, P. W., Baffaut, C., Izaurralde, R. C., Jeong, J., & Kiniry, J. R. (2012).
1106 EPIC and APEX: Model use, calibration, and validation. *Transactions of the ASABE*, 55(4), 1447–1462.

1107 WOFOST Crop Parameters: https://github.com/ajwdewit/WOFOST_crop_parameters, last access: 06 February
1108 2024.

1109 Zhang, Y., Wu, Z., Singh, V. P., He, H., He, J., Yin, H., & Zhang, Y. (2021). Coupled hydrology-crop growth
1110 model incorporating an improved evapotranspiration module. *Agricultural Water Management*, 246(1),
1111 106691. <https://doi.org/10.1016/j.agwat.2020.106691>

1112

1113

1114